JOURNAL OF PETROLEUM AND GEOTHERMAL TECHNOLOGY
ISSN: 2723-0988, e-ISSN: 2723-1496
Vol. 5 No. 1 2024

Low Salinity Water Injection Evaluation and Mature Field Development at Anggoro Shallow Sand, Sangasanga Field

Dani Novriyandi[1*)]
[1)] Petroleum Engineering, Universitas Pembangunan Nasional Veteran Yogyakarta
* corresponding email: novriyandidanidin@gmail.com

ABSTRACT

Anggoro's shallow sand was perforated at well ANG-1033 (D4-N1 layer). Oil production in this well increased from an average of 15 BOPD to 170 BOPD. That the perforated layer was affected by low salinity water injection (salinity < 3000 ppm). Evaluation of water injection sweep efficiency was carried out using the Dykstra-Parson method, vertical efficiency of about 0.3, area efficiency of 0.7, and displacement efficiency of 0.3. The Estimated Ultimate Recovery (EUR) of this well provides is 197 MBbls with an additional RF of around 20 %. This increase is due to the low salinity water injection sweep mechanism that occurs. The clay content plays an important role in the mechanism that occurs in this layer, these mechanisms fines migration, increase in pH, multi ion exchange, double layer effect, and salting in which these mechanisms result in increased oil recovery. Seeing the production results from the D4-N1 layer and oil production in this layer can still be maximized, in the future this layer can be developed with several programs such as reactivation, workover, and development drilling.

Keywords: Low salinity water injection, shallow layer, efficiency

I. INTRODUCTION

Anggoro structure is located in the Sangasanga Field, East Kalimantan. This structure is mature, indicating that oil production has declined, high water cut (around 96%), and it uses artificial lifts (ESP, SRP, HPU) to produce oil to the surface.

Water injection (waterflooding) is a secondary recovery method that is carried out in a field that has exceeded its primary recovery limit. In the Anggoro structure, water injection has been going on since 2008 with low salinity water.

The water used for injection can be distinguished based on the level of salinity, the classification can be seen in **Table 1.** below. Injection water with a salinity value below 3000 ppm is categorized as low salinity water injection.

Table 1. Water Salinity Classification (Sianturi, Julfree, 2021)

No	Classification	Salinity Range, ppm
1	Fresh water	< 1000
2	Slightly saline water	1000 – 3000
3	Moderate saline water	3000 – 10000
4	Highly saline water	10000 - 35000

Water injection with low salinity water injection is an IOR/EOR technology that increases the microscopic sweep efficiency of waterfloods by reducing and optimizing the injection water salinity resulting in a change in the wettability of the reservoir rock towards water-wet and increasing oil recovery (Parker et al., 2013).

Several parameters need to be considered in observing the effect of low salinity water injection, namely:

- Sandstone as a porous rock medium must contain a certain amount of clay which functions as a place for cation exchange to occur.
- Crude oil must contain polar acids or bases which mostly adsorb on the rock mineral surface.
- Initial formation water mainly containing divalent cations such as Ca^{2+} and Mg^{2+}.
- Increasing pH value when low salinity water are injected.
- Usually there is an increase in pressure and a decrease in rock permeability, this is related to fines migration.

This paper will discuss the positive impact of the injection of low salinity water on the Anggoro structure. The injection of low-salinity water into this structure has been going on for years.

II. METHODS

In this study, the first step was to evaluate the water injection sweep efficiency. The method used to determine the sweeping efficiency in this structure is Dykstra-Parson method.

To see the effect of low salinity water injection, we will look at the parameters described in the introduction section above. To ensure the success of injection of low salinity water in the Anggoro structure, this is confirmed by the recovery factor (RF) from observation wells.

Since water injection in the Anggoro structure gives positive results for increasing oil recovery, it is necessary to consider developing the layer that has a positive effect from low salinity water injection. It is necessary to look at the remaining reserves, drainage areas, the condition of the wells, whether there is still potential for development from a risk and economic point of view.

III. RESULTS AND DISCUSSION

Evaluation of the performance efficiency of water injection in the D4-N1 layer was carried out using the Dykstra-Parson method. Using the method, the calculation results for vertical sweeping efficiency are 0.3, area sweeping efficiency is 0.7, and displacement sweeping efficiency is 0.3. This result concludes that the sweep from water injection in this layer is quite good.

In 2018, shallow layer D4-N1 perforation job was carried out in one of the wells in the Anggoro structure, namely ANG-1033. This perforataion job is based on the results of the RMT, where it is known that the oil saturation is between 15-40%. Oil production in these wells increased from an average of 15 BOPD to 170 BOPD.

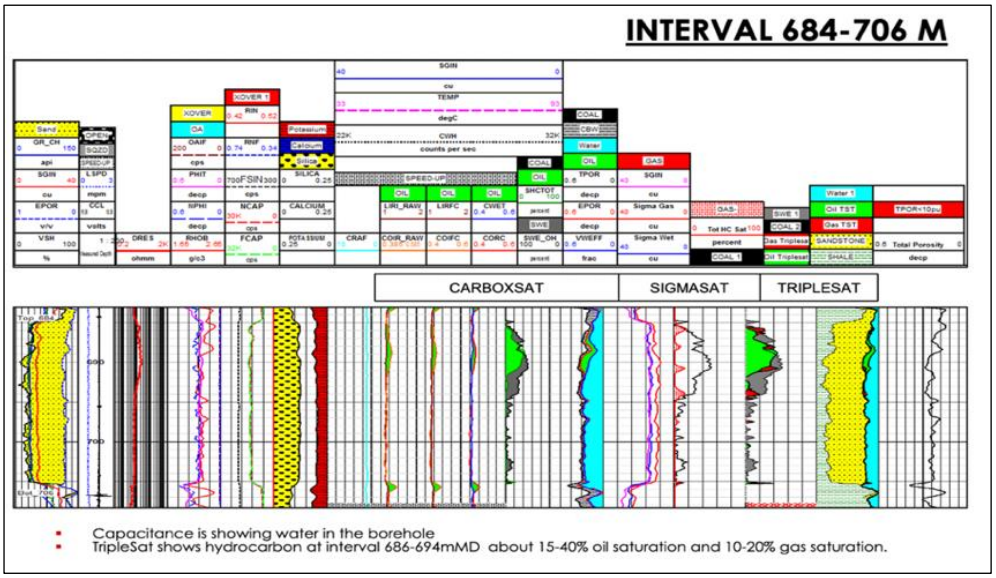

Figure 1. RMT of Layer D4-N1 in the ANG-1033 Well

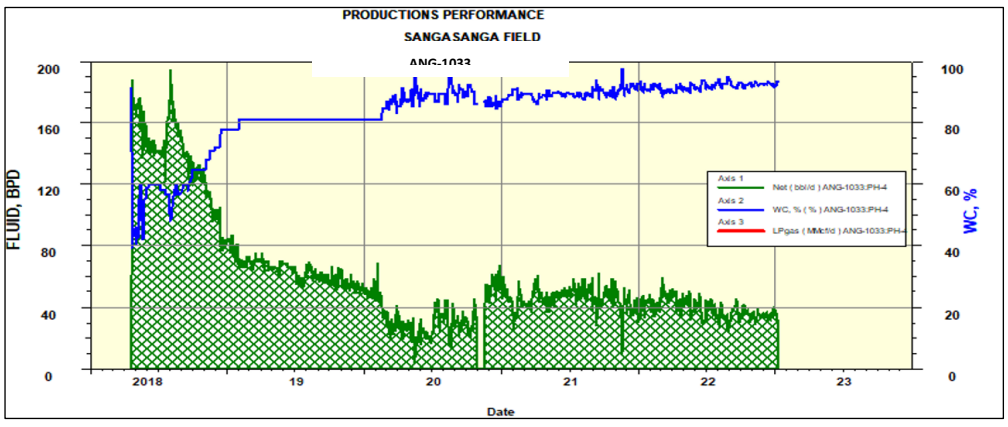

Figure 2. Production Performance of the ANG-1033 well, D4-N1 layer

JOURNAL OF PETROLEUM AND GEOTHERMAL TECHNOLOGY
ISSN: 2723-0988, e-ISSN: 2723-1496
Vol. 5 No. 1 2024

The perforated D4-N1 shallow layer is affected by the injection of low-salinity water. The injected water salinity value is quite low at 497 ppm, and the water salinity value in production wells is 284 ppm.

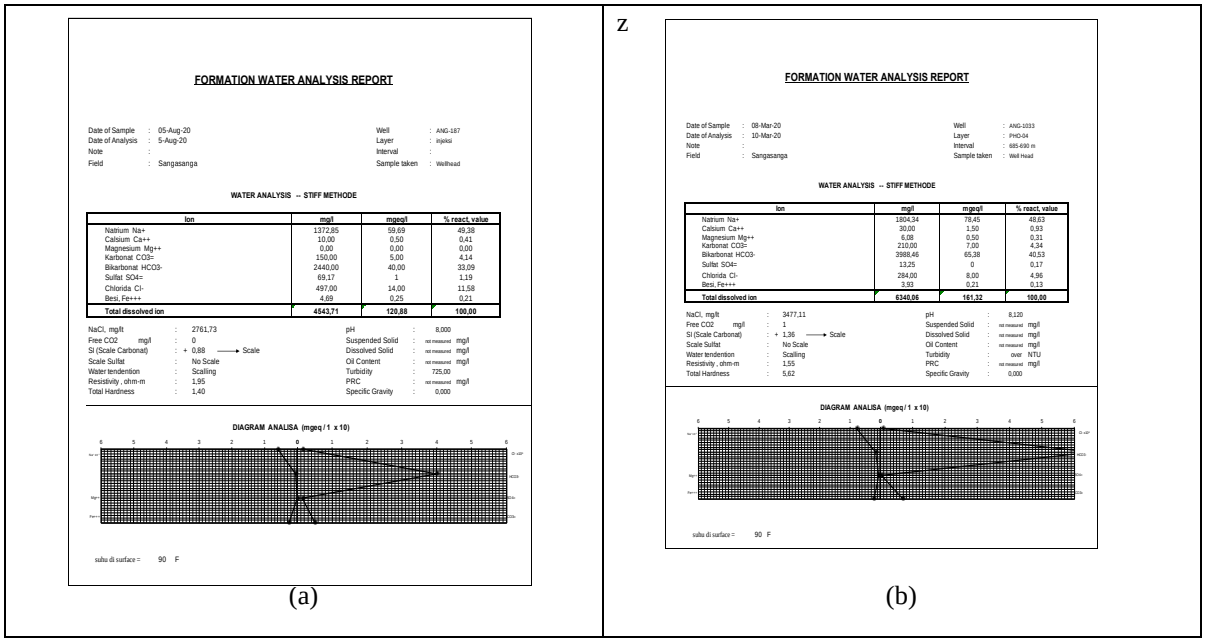

Figure 3. Laboratory Analysis of Injection Water and Production of Anggoro Structure

In addition to good sweeping, the increase in oil recovery in the Anggoro well is also due to mechanisms that occur in the rock due to the low salinity water injection. These mechanisms include:

3.1. Fines Migration

Fine particles will be released from the rock during the injection of low salinity water, and this occurs in unconsolidated sandstone. This unconsolidated sandstone occurs in shallow layers where the rock has lower overburden pressures than deeper layers.

The clay in sandstone is swelling when it reacts with low-salinity injection water, then it will cause plugging in the rock pores and will reduce fluid mobility.

3.2. pH Increase

When the water is injected with low salinity, the salt content in the rock dissolves in the water and the NaOH concentration increases, and there will be an increase in the pH value because the acid material will be absorbed by the clay surface.

An increase in the pH value will form a surfactant in-situ where it will reduce the surface tension of the oil fluid on the rock, in the sense that it will change the wettability of the rock from oil-wet to water-wet.

Formation water in the Anggoro structure during the injection of low salinity water has increased. The trend can be seen in the **Figure 4.**

3.3. Multi-ion exchange

The injection water of the Anggoro structure has Na+ cations which allow the Multi Ion Exchange mechanism to occur in the low salinity water injection system in this structure.

3.4. Double layer effect

The low salinity water injected into the Anggoro structure contains Ca2+ and Mg2+ cations. The two cations make the electrostatic bond between oil and rock very low so that the oil will easily be released from the rock.

3.5. Salting in effect

The salt content in the injection water causes an equilibrium disturbance between oil, water, and reservoir rock, causing the solubility of the oil component in the reservoir water to increase. So the oil is easier to wash off.

In the case of the ANG-1033 well, injection of low-salinity water into the D4-N1 layer can increase the recovery factor by 20%. The estimated ultimate recovery increased from 164 MBbls to 197 MBbls.

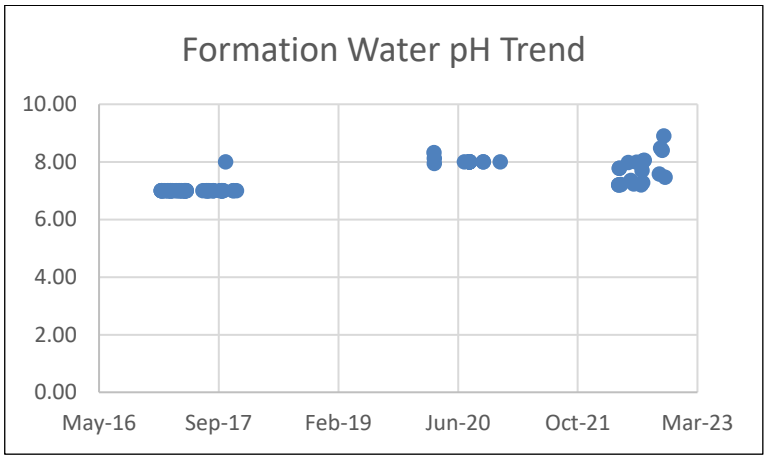

Figure 4. Trend of Formation Water pH of the Anggoro Structure

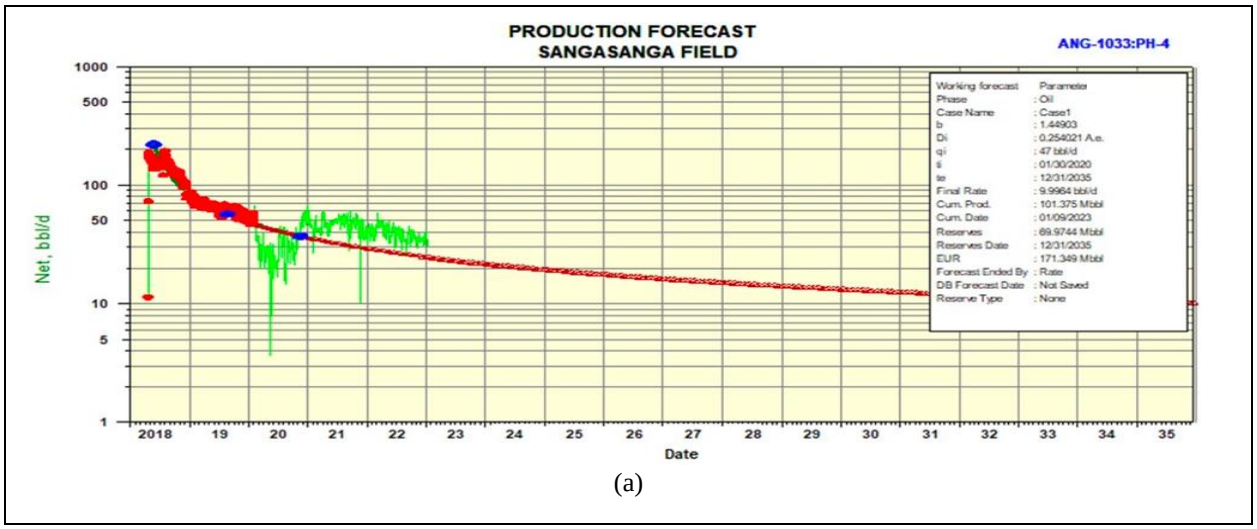

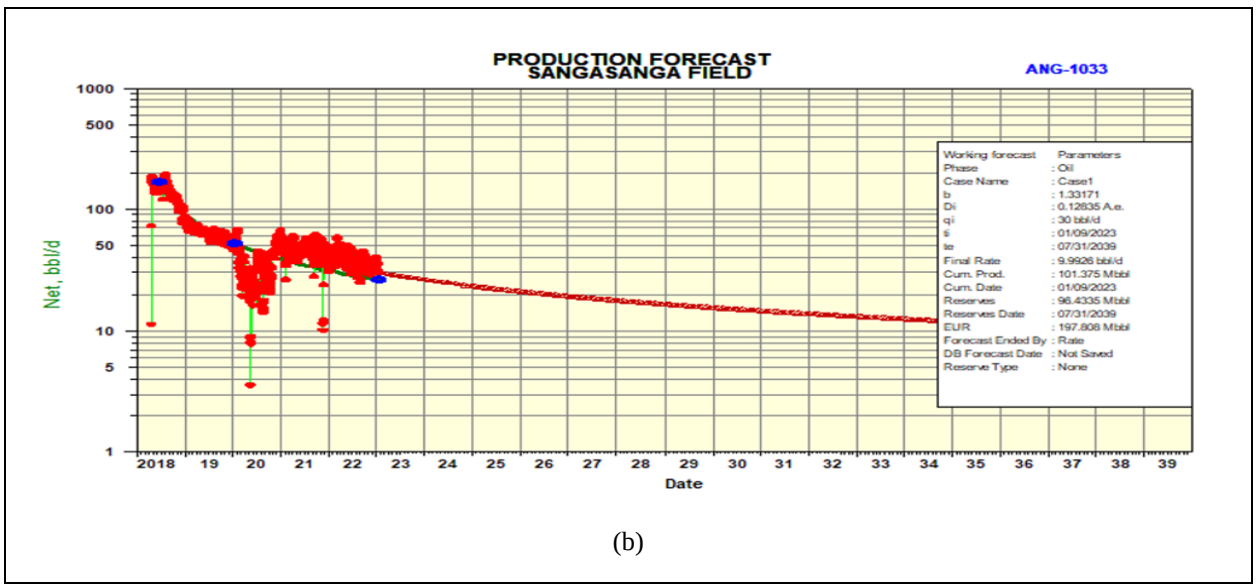

Figure 5. Decline Curve Analysis ANG-1033

Seeing the positive effects resulting from the of low salinity water injection, a study was carried out regarding the continued development plan in this D4-N1 layer. Oil cumulative and drainage radius have been revisited on this layer.

The following **Table 2.** describes the production cumulative and radius of the drainage that has occurred in this D4-N1 layer.

Table 2. Production Cumulative, Petrophysical Data and Oil Drainage Radius D4-N1 Layer

Well	Np (Mbbl)	Bo (bbl/STB)	Bw (bbl/STB)	Net Pay (m)	Net Pay (ft)	Porosity	Sw	A (Acre)	Oil Drainage Radius (Ft)	Oil Drainage Radius (m)
Blok Tengah										
ANG-175	467.976	1.08	1.002	20	65.62	0.25	0.4	18.91046	512.059	156.068
ANG-234	124.308	1.08	1.002	22	72.182	0.25	0.4	4.566515	251.6294	76.69291
ANG-236	177.378	1.08	1.002	15	49.215	0.25	0.4	9.556898	364.0219	110.9485
ANG-298	724.78	1.08	1.002	22	72.182	0.25	0.4	9.3188	359.4587	109.5577
ANG-193	843.83	1.08	1.002	20	65.62	0.25	0.4	11.93442	406.7895	123.9834
ANG-1126	4.1	1.08	1.002	14	45.934	0.25	0.4	0.082839	33.89106	10.32949
Blok Selatan										
ANG-233	322.263	1.08	1.002	27	88.587	0.25	0.4154	9.900282	370.5039	112.9241
ANG-184	54.264	1.08	1.002	13	42.653	0.25	0.4154	3.462337	219.1057	66.78016
ANG-293	468.907	1.08	1.002	23	75.463	0.25	0.4	16.47659	477.9722	145.6788
ANG-1033	100.928	1.08	1.002	23	75.463	0.25	0.4	3.546437	221.7508	67.58634
ANG-1037	97.021	1.08	1.002	22	72.182	0.25	0.4	3.564113	222.3027	67.75456
ANG-173	14.4693	1.08	1.002	8	26.248	0.25	0.4	1.461726	142.3646	43.39061
ANG-291	267.316	1.08	1.002	27	88.587	0.25	0.4	8.001467	333.084	101.5191

From **Figure 6. (a)** it can be seen that there are still several wells and areas that have not been drained optimally. To maximize the drain on this layer, several programs will be proposed including: drilling, reactivation, and workover.

The drilling program will be proposed in areas where there are absolutely no wells in the vicinity. There are 3 wells to drill in the D4-N1 layer, namely ANG-X1, ANG-X2, and ANG-X3.

The next program is reactivation, the wells that will be reactivated are wells that have previously been produced from the D4-N1 layer but the drainage radius is still small and can be maximized. Candidates for reactivation wells are ANG-123 and ANG-173.

The last program is workover that will be carried out on wells that have penetrated the D4-N1 layer but have never been produced from this layer. The wells for the workover plan are ANG-1037, ANG-1059, and ANG-1062.

Proposed wells for drilling, reactivation and workover can be seen in **Figure 6. (b).**

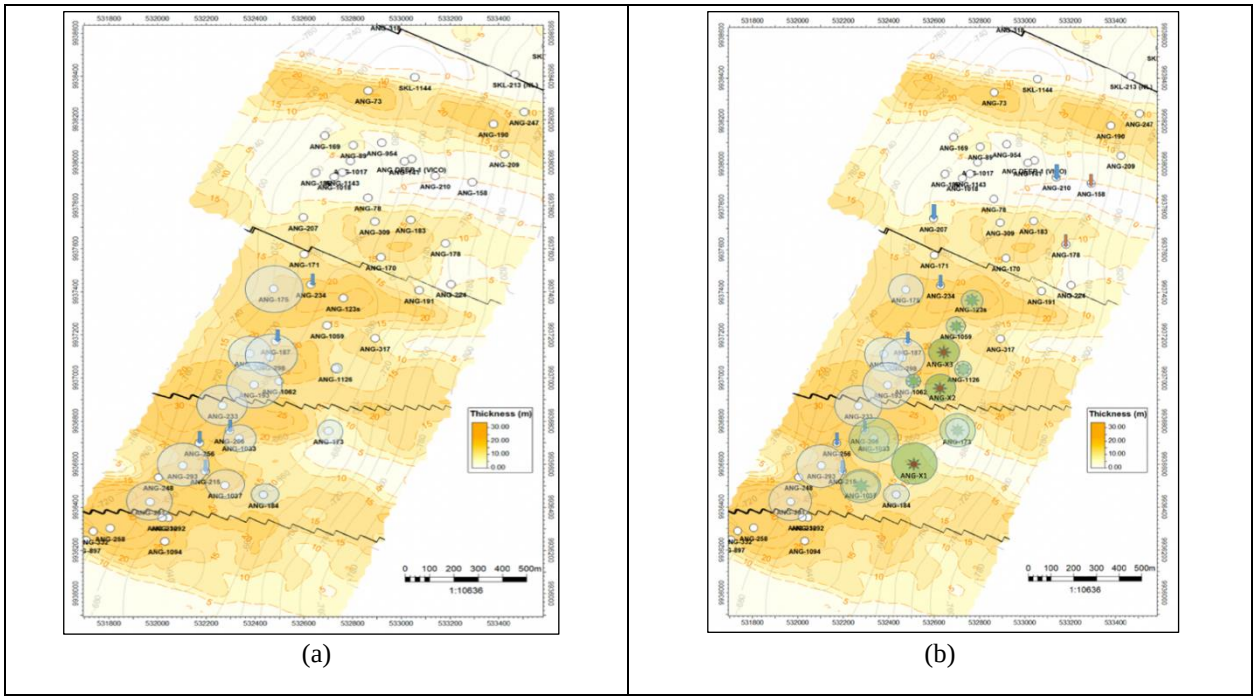

(a) (b)

Figure 6. Isopach Map and Drainage Radius of layers D4-N1

IV. CONCLUSION

1. The water injection in the Anggoro structure is low salinity water injection with a salinity value of 497 ppm and a production water salinity of 284 ppm.
2. Low salinity water injection in Anggoro structure has a positive impact on oil recovery in the D4-N1 layer (in the case of ANG-1033 well) because of the mechanisms that occur, namely fines migration, increase in pH, multi ion exchange, double layer effect, and salting in effect.
3. Oil drainage in the D4-N1 layer can still be maximized with several well work plans for future field development.
4. The work plan in the D4-N1 layer includes drilling in areas that have not been drained at all, reactivation of idle/suspended wells, and workovers at existing wells.

REFERENCES

Al-Sahiri, Abdullah; Abbas Qeinijahromi; Luis Genolet; Aron Behr; and Patrick Kowolik; Wintershal Holding; Pavel Bedrikovetsky; University of Adelaide, 2018, 'Fine Migration as An EOR Method During Low Salinity Water Flooding', SPE.

Austad, Tor; Rezaeidoust, Alireza; Puntervold, Tina; University of Satavanger, 2010, 'Chemical Mechanism of Low Salinity Waterflooding in this Sandtone Reservoir', SPE Journal.

D, Ivan; T, Pinerez; Austad, To; Strand, Skule; Puntervold, Tina; Wrobel, Stanislaw; University of Stavanger; Hamon Gerald; Total E&P; 2016, 'Linking Low Salinity EOR Effects in Sandstone to pH, Mineral Properties and Water Composition', SPE.

Morrow, Norman R, 2012, 'Low Salinity Waterflooding Fundamentals and Case Studies', IOR/EOR Conference, Wyoming.

Parker, AR, Looijer, MT, Goodyear, SG, Al-Qarshubi, ISM, Sorop, TG, Suijkerbuijk, BMJM, Dindoruk, DM, & Masalmeh, SK 2013, 'Integrated Approach in Deploying Low Salinity Waterflooding'. SPE Enhanced Oil Recovery Conference, 1–9. https://doi.org/10.2118/165277- MS

Qiao, Changhe; John Russell; LiLi; Pennsylvania State University, 2016, 'Understanding chemical mechanism for low salinity waterflooding', SPE.

Sianturi, Julfree; Bayu Setyohandoko; Aditya Suardiputra; Radya Senoputra; Pertamina Hulu Mahakam, 2021, 'Peripheral Low Salinity Water Injection Handil Case Study', IPTC.

Tang, GQ; Morrow, NR, 1999, 'Influence of Brine Composition and Fines Migration on Crude Oil/Brine/Rock Interactions and Oil Recovery', Journal of Petroleum Science Engineering.

Tarek, A, 2016, 'Reservoir Engineering Handbook (Fifth)'. Oxford, UK: Gulf Professional Publishing.

Wilhite, G Paul, 1986, 'Waterflooding', SPE textbook series vol 3.

Tetteh, Joel T; West, Rezai; University of Kansas, 2019, 'Crude-Oil/Brine Interaction as a Recovery Mechanism for Low-Salinity Waterflooding of Carbonate Reservoir', SPE Reservoir Engineering and Evaluation.

JOURNAL OF PETROLEUM AND GEOTHERMAL TECHNOLOGY
ISSN: 2723-0988, e-ISSN: 2723-1496
Vol. 5 No. 1 2024

Evaluating Cutting Transport on Route 12 ¼" Well TM-1

Ratna Widyaningsih[1*)], Ayu Utami[2)], Ristiyan Ragil[1)], Puji Hartoyo[1)], Kharisma Idea[1)], Dhika Permana Jati[1)], Pratama Dzulfiansyach[1)]

[1)] Petroleum Engineering, Universitas Pembangunan Nasional Veteran Yogyakarta
[2)] Environmental Engineering, Universitas Pembangunan Nasional Veteran Yogyakarta
* corresponding email: ratna.widyaningsih@upnyk.ac.id

ABSTRACT

Mud hydraulics on a 12-1/4" route needs to be planned properly. Mud hydraulics design on a 12-1/4" route includes determining mud density, flow type, pressure loss, pump specifications, bit hydraulics and cutting lifting design. The purpose of bit hydraulics design is to determine the optimum flow rate. Mud hydraulics optimization is carried out using methods the Bit Hydraulic Horse Power (BHHP), Bit Hydraulic Impact (BHI) and Jet Velocity (JV) methods, where the analysis is in the form of graphs. The graph is analyzed by using a trial and error method to obtain the recommended flow rate so as to provide good cutting lifting. where the expected recommendation analysis are Cutting Transport Ratio (Ft) > 90%, Cutting Concentration (Ca) < 5%, and Carrying Capacity Index (CCI) > 1. The analysis results from the graph show that for the hole 12-1/4", it is recommended to use an optimum flow rate of 626.6 gpm with minimum value of Ft is 90.01%, Ca is 0.87% and CCI is 1.95. These values are stated to be good by using 15-15-16 nozzle bit combination. The Flowrate value can be increased up to 785 gpm by using 18-18-20 nozzle bit combination.
Keywords: Hydraulic Mud Planning, Optimum Flow Rate, Cuttings Removal.

I. INTRODUCTION

The "DZ" field is located within the operational area of the Selat Malaka block and falls within the Tertiary stratigraphy of the Central Sumatra Basin. Within this field, drilling operations are planned for field development by adding an infill well, namely "TM-01," with reference data taken from offset well "SDP-28." The drilling program for well "TM-01" is scheduled to reach a depth of 2300 ftMD, targeting the sihapas formation, which consists of sandstone. This development well is designed as a vertical well.

Based on information from the reference well, the stratigraphic structure of this field is predominantly shale with hydrophilic mineral content and is also dominated by sandstone. Therefore, to facilitate an efficient and effective drilling process, the proper planning of hydraulic mud is essential to ensure optimal removal of cuttings from the wellbore.

The hydraulic mud planning for well "TM-01" is intended for two trajectories, namely the 12-1/4" and 8-1/2" trajectories. The planning process involves several stages, including data collection, data processing, planning, optimization, and evaluation. The ultimate objectives of this hydraulic mud planning are twofold. Firstly, it aims to determine the optimum flow rate values and identify the optimal nozzle size combinations suitable for the geometrical conditions of each trajectory. Secondly, it aims to achieve good hole cleaning criteria after optimizing hydraulic mud, taking into consideration the cutting transport ratio (Ft) above 90%, cutting concentration (Ca) below 5%, and carrying capacity index (CCI) above or equal to 1 (Wastu et al., 2019).

If the minimum criteria for these three parameters are met, it can be concluded that the level of cuttings removal after hydraulic planning is considered satisfactory. Improved hole cleaning directly impacts the rate of penetration (ROP), which in turn enhances drilling efficiency by reducing drilling time.

II. METHODS

The research methodology employed in the study of Hydraulic Mud Drilling Planning for Well "TM-01" in the "DZ" field encompasses several phases. These include data collection and processing from the offset well 'SDP-28,' encompassing data such as pore pressure fracture gradient, hole diameter geometry, depth, drill string diameter and length, casing design, drilling parameters such as Rate of Penetration (ROP), Rotation Per Minute (RPM), offset well flow rate, mud data such as density and cutting size, Plastic Viscosity (PV) dan Yield Point (YP).

The determination of mud density for each trajectory based on the drilling window of the reference well. This phase is carried out by plotting the formation pressure and formation fracture pressure values against drilling depth on a single graph to ascertain the upper and lower boundary safety factors for establishing the safe mud weight for each trajectory for well "TM-01." Determining the type of mud flow occurring within the drill string and annulus for each trajectory. To

ascertain whether mud flow will be laminar or turbulent, various parameters, including dial readings from the viscometer (θ600, θ300, θ200, θ100, θ6, and θ3), are necessary to obtain PV and YP. Additionally, data on flowrate, inside and outside drill string diameters, and length of the offset well's drill string significantly influence the determination of mud flow type.

This analysis will utilize a modified-power law or Herschel-Buckley fluid model, as employed in the offset wells. Determining the magnitude of parasitic pressure loss occurring within the drill string and annulus for each trajectory and subsequently planning the bit pressure loss, which is then added to the parasitic pressure value to determine the pump pressure required for mud circulation. Planning pressure loss is crucial for establishing the pump pressure specification that aids in optimizing hydraulic mud. Determining the pump specifications capable of meeting the required pump pressure. In this phase, the required pump specifications include maximum HP pump, maximum pump pressure, and displacement pump. Determining the maximum flow rate as the upper limit to prevent mud turbulence. The determination of the maximum flow rate is calculated based on the pump specifications that will be used, considering parameters such as horsepower, pump pressure, and utilized flow rate. This implies that the maximum pump capacity will provide the required maximum flow rate without inducing turbulence.

Determining the minimum flow rate as the lower limit for cutting suspension. When establishing the minimum flow rate, values for annular velocity and slip velocity are obtained, closely related to how mud can suspend cuttings to prevent settling when mud is in dynamic conditions. Additionally, parameters such as cutting concentration and minimum velocity also influence the determination of the minimum flow rate. Planning hydraulic mud optimization to maximize mud flow rates based on the BHHP, BHI and JV methods, resulting in optimal flow rates and nozzle combinations. Through these three methods, various optimal flow rates with suitable nozzle combinations are determined. For BHHP, it maximizes the surface power potential used by the bit. For BHI, this method maximizes the impact potential of the mud exiting the nozzle against the rock. For jet velocity, it maximizes the nozzle jetting potential by maximizing the surface pump rate, thereby achieving maximum bit rate. Analyzing the success rate of hole cleaning after obtaining the optimum flow rate using several cuttings removal methods such as Cutting Transport Ratio (Ft), Cutting Concentration (Ca), and Carrying Capacity Index (CCI). According to (Al Rubaii, 2018), cuttings removal analysis can be conducted through three methods: cutting transport ratio (Ft) with a value exceeding 90%, cutting concentration ranging from 5-8%, and carrying capacity index with a value of 1.

III. RESULTS AND DISCUSSION

This drilling operation is conducted for field development by adding an infill well, namely "TM-01," utilizing reference data from the offset data well "SDP-28." The drilling program for well "TM-01" is planned to reach a depth of 2300 ft-MD, targeting the Sihapas Formation, which comprises sandstone reservoirs. This development well is of the vertical well type. By conducting hydraulic mud planning based on the reference well, it is expected that the planning results will positively influence cuttings removal and wellbore cleaning by meeting hole cleaning parameter criteria such as Ft, Ca, and CCI. For the 12-1/4" trajectory, drilling commences from a depth of 155 ft-MD and will penetrate through shale layers until casing installation of 9-5/8" from the surface down to a depth of 1250 ft-MD to isolate these shale layers.

Further data required for hydraulic mud drilling planning includes bit data, Bottom Hole Assembly (BHA) data, and drill string data. For well 'TM-01,' a Polycrystalline Diamond Compact (PDC) type bit will be utilized with specifications as outlined in **Table 1**. BHA and drillstring configurations will be based on reference data from well 'SDP-28.' There are two types of BHA and drillstring configurations, each for the 9-5/8" and 7" trajectories, generally consisting of drillstring equipment such as drillpipe, Heavy Weight Drill Pipe (HWDP), drill collar, drill jar, crossover sub, stabilizer, and bit sub. The drillstring data tabulation is provided for the 12-1/4" trajectory.

After conducting calculations for the 12-1/4" trajectory in well "TM-01," it was found that the cuttings removal results using the optimum flow rate based on the actual nozzle configuration were not entirely optimal. Therefore, a trial and error approach was employed to determine the optimum flow rate from the results of the optimization of three hydraulic bit methods through graphical plotting. The ultimate goal is to provide recommendations for the nozzle and the optimal flow rate range that meet the minimum criteria of the three cuttings removal methods: Ft, Ca, and CCI. For the 12-1/4" trajectory, it is recommended to use the optimum flow rate with a minimum cuttings removal value considered good at 626.6 with a bit nozzle combination of 15-15-16. The flow rate can be increased up to 785 gpm with a nozzle combination of 18-18-20. It is also known that using the actual nozzle results in poor cuttings removal. The "DZ" field is located in the working area of the Malacca Strait block and is still within the tertiary stratigraphy of the Central Sumatra Basin. In this field, drilling will be carried out for field development by adding an infill well, namely "TM-01," using reference data from the offset well "SDP-28." This development well is of the vertical well type.

Table 1. Tabulation of BHA Data for the 12-1/4" Trajectory

BHA 12-1/4"					
No.	Description	OD	ID	Length, ft	Total Length, ft
		in	in		
1	5" DP CSG	5.00	4.28	155.00	155
2	5" DP OH	5.00	4.28	684.82	839.82
3	5" HWDP	5.00	3.00	30.95	870.77
4	5" HWDP	5.00	3.00	31.10	901.87
5	5" HWDP	5.00	3.00	30.83	932.70
6	5" HWDP	5.00	3.00	30.95	963.65
7	5" HWDP	5.00	3.00	31.07	994.72
8	5" HWDP	5.00	3.00	30.84	1025.56
9	6-1/2" DC	6.50	3.00	30.75	1056.31
10	6-1/2" DC	6.50	3.00	28.84	1085.15
11	6-1/2" Drill Jar	6.50	3.00	31.97	1117.12
12	6-1/2" DC	6.50	3.00	30.02	1147.14
13	6-1/2" DC	6.50	3.00	29.98	1177.12
14	8" X/O	8.00	3.00	1.64	1178.76
15	8" DC	8.00	3.00	31.07	1209.83
16	12-1/4" Stab	12.00	3.00	5.18	1215.01
17	8" DC	8.00	3.00	30.74	1245.75
18	8" Bit Sub	8.00	3.00	3.00	1248.75
19	12-1/4" PDC bit	12.25		1.25	1250.00
BHA TOTAL				410.18	

Table 2. Bit Data

Bit					
Bit Size	Casing Size	Merk	Type	*Nozzle*	d *Nozzle* (in/32)
Driven	13.375		-	-	
12.25	9.625	NOV RH	PDC	7 x15	0.46875

Table 3. Drilling Powder Data

Data *Cutting*			
Hole	Diameter (mm)	Diameter (in)	Densitas (lb/gal)
12-1/4"	3.5	0.137795276	19.992

Table 4. Mud Properties Data 12-1/4”

12-1/4"							
θ600	θ300	θ200	θ100	θ6	θ3	PV	YP
63	43	27	13	6	4	20	23

The "DZ" field is located in the working area of the Malacca Strait block and is still within the tertiary stratigraphy of the Central Sumatra Basin. In this field, drilling will be carried out for field development by adding an infill well, namely

"TM-01," using reference data from the offset well "SDP-28." This development well is of the vertical well type. Preparations have been made for the drilling program, including hole geometry, casing design, and the drillstring to be used. Therefore, hydraulic mud planning is required for this well to facilitate a smooth drilling process. The drilling program for well "TM-01" is planned to reach a depth of 2300 ftMD, targeting the sihapas formation, which consists of a sandstone reservoir. This well will be divided into three trajectories: the 13-3/8" trajectory with conductor casing installation from 0 ftMD to 155 ftMD, the 12-1/4" trajectory with surface casing of 9-5/8" from 0-1250 ftMD, and the 8-1/2" trajectory with production casing of 7" from 0 to 2300 ftMD.

The planning of hydraulic mud is required for the 12-1/4" and 8-1/2" trajectories. This planning includes the determination of mud density, the determination of flow type, the determination of pressure loss, the determination of pump specifications, hydraulic bit planning to determine the optimum flow rate, and cuttings removal planning.

Data collection is carried out from the offset well 'SDP-28,' including well data such as depth and hole geometry. Drilling parameter data, such as the planned drillstring and BHA configuration, drillstring and BHA diameter measurements, pump data, bit data, pressure window data, and drilling mud data, such as mud properties like dial readings of θ600, θ300, θ200, θ100, θ6, and θ3, PV and YP values, density, and cutting diameter.

The first step in hydraulic planning is to determine the mud window, which aims to establish a safe mud weight that does not cause drilling problems. To determine the mud window, pressure window data such as formation pressure and fracture pressure are required. Since well "TM-01" is still within the same contour as the reference well, pressure data can be used as a reference for determining the mud window. Mud weight determination is carried out for two trajectories, 12-1/4" and 8-1/2". For the 12-1/4" trajectory, a mud weight of 9.6 ppg will be used, and for the 8-1/2" trajectory, a mud weight of 10 ppg will be used. These values include safety margins added to the formation pressure. At this stage, the Equivalent Circulating Density (ECD) magnitude is also determined, where the mud conditions, when dynamic and carrying cuttings, experience an increase in density. The determination of the ECD value is necessary for calculating the total annulus pressure loss, which reveals the increase in mud weight under static conditions. For the 12-1/4" trajectory, the ECD value ranges around 10.7 ppg, and for the 8-1/2" trajectory, it ranges around 10.9 ppg. These values remain below the fracture pressure, ensuring that the mud weight does not pose drilling problems.

Before determining the flow type, it is important to understand the rheology model of the drilling mud being used. In this well, the fluid model employed is Herschel-Bulkley after plotting shear rate against shear stress, obtained through dial reading on the viscometer. This fluid rheology applies to both trajectories. After determining the rheology of the mud, parameters derived from the Herschel-Bulkley fluid type, such as yield stress, Herschel-Bulkley flow index, and Herschel-Bulkley consistency index, are required to determine the flow type and other aspects. For the 12-1/4" trajectory, the yield stress ($\tau\gamma$) was found to be 2, with a flow index value of 0.5732 and a consistency index value of 574.50 cp. Once these parameters are obtained, the next step is to determine the flow type that occurs during circulation. The determination of the flow type is based on the critical Reynolds number (Nrec) value. If the Reynolds number (Nre) of a flow exceeds the Nrec value, the flow is considered turbulent. Conversely, if the Nre of a flow is less than the Nrec value, the flow is considered laminar. To calculate the Nrec value, values of γ and z, which are 0.0737 and 0.284, respectively, are needed. Thus, the Nrec values for the drillstring are 2338.67, and for the annulus, they are 4426.2.

The determination of the flow type will be divided into several sections, with each section having different borehole geometry conditions depending on the diameter of the mud flow. It was found that the Reynolds number along the flow inside the drillstring is turbulent, while the flow inside the annulus is laminar. This is considered favorable because within the drillstring, turbulent flow is necessary to ensure that the power delivered by the pump is not lost before reaching the bit, and turbulent flow exiting the bit can cause abrasion, preventing cuttings from settling. In contrast, laminar flow is desired in the annulus due to the borehole conditions that have not been cased, and the mud's function is to provide a mudcake on the borehole wall to withstand formation pressure. After determining the fluid flow type, the next step in mud hydraulic planning is to calculate the magnitude of pressure loss that occurs during mud circulation. The goal is to determine the value of equivalent circulating density and ascertain the pump pressure required at the actual flow rate. The calculation of the minimum pump pressure is identical to the calculation of pressure loss in the circulation system, except at the bit, which represents parasitic pressure loss. To determine the required pump pressure, the total pressure loss value is calculated. To obtain the total pressure loss, it comprises the sum of parasitic pressure loss and bit pressure loss. Parasitic pressure loss represents the total pressure loss that occurs in the drillstring except at the bit, both inside and outside the annulus. The parasitic pressure loss for the 12-1/4" trajectory is 484.28 psi. Once the parasitic pressure loss value is obtained, the next step in mud hydraulic planning is to determine the magnitude of pressure loss that occurs at the bit. In the 12-1/4" trajectory, a 12.25-inch PDC bit with a nozzle size of 7x15 is used. The nozzle Discharge Coefficient (Cd) is set at 0.95. To calculate the pressure drop at the bit, the area produced by the nozzle diameter is required. With the given nozzle diameter, the area of the nozzle is 0.5177 square inches. The pressure loss at the bit is found to be 1116.49 psi. Therefore, in the 12-1/4" trajectory, the total pressure loss amounts to 1600.787 psi. Therefore, a pump capable of providing a minimum pressure of 1600 psi is required.

Therefore, the pump selected for well 'TM-01' in the 12-1/4" trajectory is the Oilwell A600-PT, which is a triplex pump. Three pumps are employed, with two active pumps and one backup pump, configured in parallel, with a maximum HP of 1080 hp, a maximum flow rate of 849.6 gpm, and a maximum pressure of 1767 psi. Subsequently, the determination of the minimum flow rate is required to establish the minimum limit at which cutting can remain suspended in the mud. To calculate the minimum flow rate, the concept of Vmin or minimum velocity is utilized. During this stage, values for annular velocity, apparent viscosity, slip velocity, cutting velocity, minimum velocity, and minimum flow rate are determined. For the 12-1/4" trajectory, a minimum flow rate of 292.13 gpm is needed.

IV. CONCLUSION

Through the hydraulic design of well "TM-01" for the 12-1/4" trajectory, the hydraulic bit design using the actual nozzle configuration of 15-15-15 yielded an optimum flow rate of 600 gpm with cuttings removal results of Ft 89.6%, Ca 0.9%, and CCI 1.86. The cuttings removal is considered poor. In the course of planning the drilling of well "TM-01," various aspects of hydraulic mud have been meticulously considered. A safe mud weight has been determined, taking into account formation and fracture pressures, including the addition of safety margins. The type of mud flow in the well has been analyzed using the Herschel-Bulkley rheology model, resulting in turbulent flow within the drillstring and laminar flow within the annulus. Calculating pressure losses is essential to determine the required pump pressure, considering parasitic pressure and pressure loss at the bit. The precise selection of the Oilwell A600-PT pump is made to meet the minimum pressure requirements for mud circulation. Lastly, the minimum flow rate required has been calculated to ensure that cuttings remain suspended in the mud. With this thorough planning, it is anticipated that the drilling of well "TM-01" can be executed with maximum efficiency and safety to achieve the targeted depth.

REFERENCES

Adam, N. J., & Charrier, T. (1985). Drilling Engineering, A Complete Well Planning Approach.

Al Rubaii, M. M. (2018). A new robust approach for hole cleaning to improve rate of penetration. Society of Petroleum Engineers - SPE Kingdom of Saudi Arabia Annual Technical Symposium and Exhibition 2018, SATS 2018, April 2018. https://doi.org/10.2118/192223-ms

Baker Hughes. (2006). Drilling Fluids Reference Manual. Reference Manual, 1– 775.

Bieler, R. (1990). Selecting a Drilling Fluid. July, 832–834.

Bourgoyne, J. A. T., Keith, K. M., Martin, E. C., & F.S., Y. J. (1986). Applied Drilling Engineering SPE (p. 500). https://store.spe.org/Applied-Drilling- Engineering-Digital-Edition-P576.aspx

Busahmin, B., Saeid, N. H., Alusta, G., & Zahran, E. S. M. M. (2017). Review on hole cleaning for horizontal wells. ARPN Journal of Engineering and Applied Sciences, 12(16), 4697–4708.

Busahmin, B., Saeid, N. H., Hasanah, U., Hj, B., & Alusta, G. (2017). Analysis of Hole Cleaning for a Vertical Well. 4. https://doi.org/10.4236/oalib.1103579

Caenn, R., & Chillingar, G. V. (1996). Drilling fluids: State of the art. Journal of Petroleum Science and Engineering, 14(3–4), 221–230. https://doi.org/10.1016/0920-4105(95)00051-8

Dr. Ir. Rudi Rubiandini R.S., I. (2009). Teknik Pemboran 1. 417–444.

Exlog. (1985). Theory and Application of Drilling Fluid Hydraulics (Vol. 4, Issue 1).

Guo, B., & Liu, G. (2011). Applied drilling circulation systems: Hydraulics, calculations and models. In Applied Drilling Circulation Systems: Hydraulics, Calculations and Models. https://doi.org/10.1016/C2009-0-30657-1

Herianto. (2021). Optimization Rate of Penetration in Directional Drilling with Adjustable Bit Rotating and Hydraulic Hole Cleaning. 9(5). https://doi.org/10.14738/aivp.95.11097

Herianto, & Subiatmono, P. (2021). Teori dan Aplikasi Pemboran Berarah Pada Sumur Minyak dan Gas.

Julikah, J., Rahmat, G., & Wiranatanegara, M. B. (2021). Subsurface Geological Evaluation of the Central Sumatra Basin in Relation to the Presence of Heavy Oil. Scientific Contributions Oil and Gas, 44(1), 65–81. https://doi.org/10.29017/scog.44.1.491

Mahmoud, H., Hamza, A., Nasser, M. S., Hussein, I. A., Ahmed, R., & Karami, H. (2020). Hole cleaning and drilling fluid sweeps in horizontal and deviated wells: Comprehensive review. Journal of Petroleum Science and Engineering, 186, 106748. https://doi.org/10.1016/j.petrol.2019.106748

Okon, A. N., Agwu, O. E., & Udoh, F. D. (2015). Evaluation of the cuttings carrying capacity of a formulated synthetic-based drilling mud. Society of Petroleum Engineers - SPE Nigeria Annual International Conference and Exhibition, NAICE 2015, September. https://doi.org/10.2118/178263-ms

Rabia, H. (2002). Well Engineering & Construction Hussain Rabia. 1 to 789. Subraja, T., Lestari, L., Husla, R., Apriandi, R. R. W., & Yasmaniar, G. (2022).

Analisa Pengangkatan Cutting Menggunakan Metode CCI,CTR, Dan CCA Pada Sumur T Trayek 17 1/2". XI(1), 6–11.

Texaco, C. (2002). The Chevron Texaco and BP Drilling Fluid Manual.

Wastu, A. R. R., Hamid, A., & Samsol, S. (2019). The effect of drilling mud on hole cleaning in oil and gas industry. Journal of Physics: Conference Series, 1402(2). https://doi.org/10.1088/1742-6596/1402/2/022054.

JOURNAL OF PETROLEUM AND GEOTHERMAL TECHNOLOGY
ISSN: 2723-0988, e-ISSN: 2723-1496
Vol. 5 No. 1 2024

Overcoming the Sand Problem Using the Gravel Pack Method in Well X in the Field of Kalrez Petroleum (Seram) Ltd

Wa Riska Lanongko[1*)]
1) Oil and Gas Production Engineering, Ambon State Polytechnic
* corresponding email: riskakim180@gmail.com

ABSTRACT

In the oil and gas industry, there are often various problems that can interfere with the production process. One of the problems that often occurs is sand problems. The impact of sand problems is to cause damage to downhole and surface equipment. To solve the problem of sand in boreholes, gravel fill can be used. This study was conducted Kalrez Petroleum (Seram) Ltd Field Well X. The purpose of this study was to determine the size of gravel Bagging overcomes sandy issues and determines front and rear production performance Installing a gravel pack and determining the cost comparison of the gravel pack method and sand screening method in terms of cost benefit analysis. Based on the smallest average size of sand grains is 0.024 inch, this size is in accordance with the size of gravel pack in general, namely 16/30 M. Calculation of PI after the use of gravel pack has increased production from 4.4 bbl/psi to 7.8 bbl/psi. Based on the IPR curve before the use of gravel pack, the maximum flow rate (Q max) was 527.4372 bpd, experiencing an increase in the maximum flow rate (Q max) of 907.108 bpd. Based on calculations using cost benefit analysis (Coast Benefit Analysis) between the gravel pack and screen liner methods. The screen liner method can be an alternative to overcome the sand problems, this is because it is seen from the value of the B/C ratio> 1 or 2,3. This means that for every one dollar invested in the method, a savings ratio of 2.3 will be obtained. So the screen liner method is more useful and also efficient.
Keywords: Sand problem, downhole and surface equipment, gravel pack, sieve analysis, cost benefit analysis

I. INTRODUCTION

The problem of sand production is one of the problems encountered by the oil and gas industry, especially the upstream of the oil and gas industry (Roslan, et, 2010). Oil and gas companies spend millions of dollars each year to prevent and solve sand problems Problems in unconsolidated formations result in lost production and damage to well equipment (Hisham, 2015).

According to data obtained from Kalrez Petroleum (Seram) Ltd, the oil field is an old oil field that has been operating since 1939, so there are many problems in the oil wells in this field, and the most common problem is the problem of passivity. In the X well of the Kalrez Petroleum (Seram) Ltd field, the potential for the occurrence of sand is very high, causing the production of crude oil from year to year to decline. Sand production usually comes from younger tertiary reservoirs, such as Miocene and Pliocene aged sands. These sands are usually unconsolidated sand layers that are highly susceptible to changes in reservoir pressure as well as water coning, which can cause sandiness problems (Bergkvam, 2015). Sand production is highly undesirable during production activities because it can cause many problems both in the surface facility and downhole equipment.

The mechanism that causes the siltation problem starts with the production rate exceeding the critical flow rate, leading to water breakthrough (Ahmed, 2006). In the reservoir production zone, with low rock compaction and poor rock bonding and cementation, it is susceptible to contact with formation water, which causes the clay content to swell and weaken. Thus, the bonds between the rock grains are released along with the reservoir fluid during well production (Isehunwa & Farotade, 2010). In addition, decreasing reservoir pressure can also lead to the occurrence of passivation problems where, when reservoir pressure decreases, it will affect the increase in overburden pressure which causes weakening of rock cementation (Mayokun A. O., 2011). One way to overcome the problem of passivity is by using mechanical methods, namely gravel packs.

Overcoming the problem of sandiness with the gravel pack method is by installing gravel that is inserted into the borehole so that it can prevent the entry of sand grains into the production hole or production well. The selection of gravel size must be adjusted to the condition of the rock grains. Therefore, in determining the size of gravel, the right design is needed. In this study, the data source comes from the Kalrez Petroleum (Seram) Ltd field located in Bula, in addition to using economic analysis to choose a method of overcoming sandiness.

The formulation of the problem in this research thesis is to understand the problem of passivity, determine the size of gravel pack used to overcome the problem of passivity, production performance before and after gravel pack installation, cost benefit analysis that occurs in the X well field of Kalrez Petroleum (Seram) Ltd. This research was conducted to be able to understand the problem of passivity, determine the size of gravel pack used to overcome the problem of passivity, production performance, and cost benefit analysis at the X well of the Kalrez Petroleum (Seram) Ltd. field.

In the concluding section of the introduction, the research's objectives or aims should be articulated. These objectives should be highlighted in the literature review to underscore the novelty of the scientific article.

II. METHODS

In this research, there are several stages used by the author in this research methodology:

1. Study Literature
   Is the initial stage carried out by searching for information both from supporting books, journals, theses and papers related to the research being conducted.

2. Data Collection
   Is taking the data needed in the research preparation process. Data collection is done by requesting data and discussing with field supervisors regarding matters related to research.

3. Data Processing
   a. Determine Sand Grain Size
      Determined from sieve analysis obtained from formation sand samples. Sieve analysis begins with
      - Preparing formation sand samples that have been dried and free from oil
      - Prepare a sieve analysis whose bottom has been cleaned, the sieve is arranged above the shaker and above the bowl at its base
      - Set the sieve starting from the finest at the top of the bowl and the coarsest at the top.
      - Pour the formation sand sample into the top sieve, attach the cover securely and shake for 30 minutes.
      - Pour the formation sample in the topmost sieve into a container and weigh it and continue to the next sieve layer.
      - Weigh the cumulative weight of the formation sample using a digital balance.
      - Make a semilog graph between opening diameter and cumulative %

   b. Gravel Pack Size
      Determining the size of the gravel pack is done after obtaining the sieve analysis data which then plots the sample data results on the opening diameter and also the cumulative % so as to get the sorting coefficient so that it can determine the size of the gravel pack. The graph between opening diameter and cumulative % is done with the equation

      $$\text{Uniformity Coefficient} = \frac{(\text{Diameter at } 40\%)}{(\text{Diameter at } 90\%)}$$

   c. Calculating PI and IPR
      In this step the author analyzes the production performance before and after the installation of gravel packs using PI and IPR calculations.

   d. Cost Benefit Analysis
      At this stage, the author can compare the costs that have been invested in the development of the benefits or profits obtained by Kalrez Petroleum (Seram) Ltd.

III. RESULTS AND DISCUSSION

3.1. Sand Problems in Well X of Kalrez Petroleum (Seram) Ltd Field

During production activities, the problem that often occurs is the production of sand to the surface, which can affect the productivity of the well. Sand formations generally contain clay or cement rock as well as clay. Clays have a characteristic called water wet, so when water flows through rock layers containing clays, there is a tendency for sand particles to migrate towards the wellbore when produced water is produced.

The production of sand to the surface along with the fluid is one of the problems that often occurs in the Kalrez Petroleum (Seram) Ltd field such as in the X well. This well uses an artificial lift method using a sucker rod pump. Where this pump is less than optimum for handling sand problems. With the condition of the well like this so that to handle the problem of sandy needs special handling, namely by using the gravel pack method so that the sandy problem can be handled.

3.2. Size of Gravel Pack Used

To determine the size of sand grains in the X well of Kalrez Petroleum (Seram) Ltd, a core analysis using sieve analysis is carried out, where sieve analysis is an analysis carried out on the size of sand grains to select the size of sand grains and also gravel packs or determine the weight presentation of grains that pass a set of sieves.

Table 1. Sand Grain Size Distribution

Grain Size		% Weight	% cumulative
Mesh	Inchi		
20	0,0331	0,471	0,471
30	0,0232	0,548	1,019
35	0,0197	0,430	1,450
50	0,0117	2,771	4,221
60	0,0098	11,466	15,687
80	0,0070	23,400	39,087
100	0,0059	44,548	83,635
200	0,0029	15,741	99,376
>200	0	0,624	100

Before determining the size of gravel pack to be used, first know the distribution of sand grain size in the well. By analyzing the size of sand grains, it can determine the selection or sortation (C).

The results of core analysis using sieve analysis of sand from well X, in the sample above illustrates the particle size distribution of sand expressed in terms of weight percentage of each particle size. The sample data is then plotted into a semilog graph shown in the figure below.

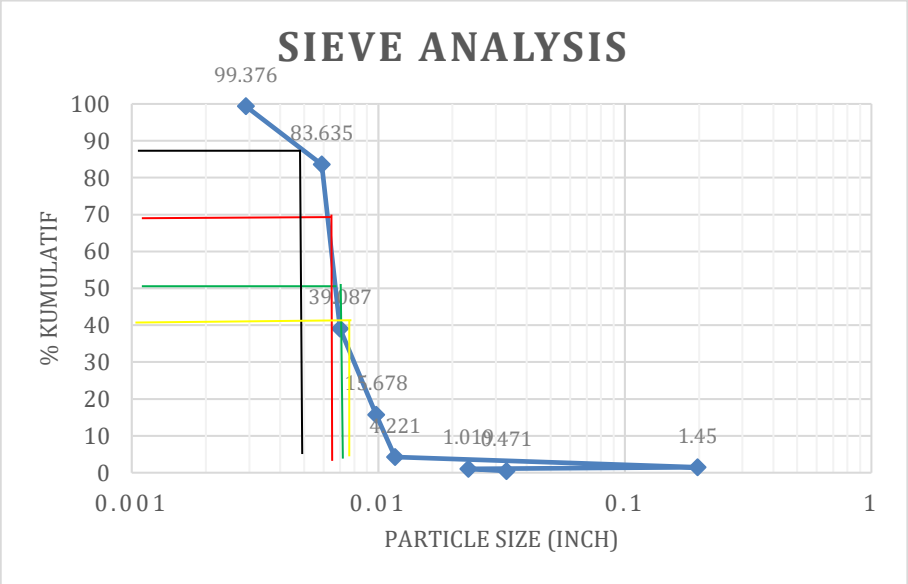

Figure 1. Cumulative vs Particle Size

From the curve, the percentage of sand grain size can be determined. To determine the percentage value, the most dominant distribution can be selected, as shown in the table below:

Table 2. Most Dominant Sand Grain Size Distribution

Persent, D	Ukuran, Inch
D40	0,0088
D50	0,0086
D70	0,007
D90	0,004

After determining the size of the sand distribution as in the table above, the next stage is to determine the uniformity of the sand grains.

3.3. Determining Sand Grain Uniformity

The Coefficient of Uniformity is calculated by comparing the sand grain size at the 40% percentile (D40) with the sand grain size at the 90% percentile (D90). The equation is as follows:

From the Percent Result, determine the uniformity of sand grains.
If known:

D40 = 0,0088
D90 = 0,004
Answer:

$$\text{Uniformity Coefficient} = \frac{\text{Diameter at 40\%}}{\text{Diameter at 90\%}} = \frac{0{,}0088}{0{,}0024} = 2{,}2$$

Based on the sand grain size consistency calculations that have been carried out, it can be observed that the Coefficient of Uniformity (C) value is lower than 3 (C < 3). Therefore, it can be concluded that the sand grain size is classified as good or uniform.

Table 3. Selection of Good, Medium, Poor, Sand Grain Size According to Schwartz

C = d40/d90	Sorting
C < 3	Well sorted
C < 5	Moderately sorted
C > 5	Poorly sorted

3.4. Determining Gravel Pack Size

To determine the gravel pack size to solve the sand problem in well X, the authors used the Schwartz approach. This approach involves the selection of gravel pack size based on sand particle size. This method involves the use of a formula where the gravel pack size is determined by multiplying 6 times the diameter of the sand particles at the 40% percentile (6 x D40) and 90% percentile (6 x D90). Details of the results are provided in the table below:

Table 4. Schwartz Method 6× Formation Sand Size

Percent	Size, inch	6×
40%	0,0088	0,0528
50%	0,0086	0,0516
70%	0,007	0,042
90%	0,004	0,024

Table 5. Gravel Pack Size

Size Range, Inch	Gravel Size, U.S. Mesh
0,066-0,094	8/12
0,033-0.066	12/20
0,023-0,047	16/30
0,017-0,033	20/40
0,010-0,017	40/60

From the table above, the smallest gravel pack size is 0,024, thus, this size corresponds to the size generally used for gravel packs, which is 16/30 US Mesh.

3.5. Production Performance Before and After Gravel Pack Installation

To determine the production performance before and after the installation of gravel packs, the production data in the table below is used.

Table 6. Production Data Before and After Gravel Pack Installation

Production Data	Before Gravel Pack Installation	After Gravel Pack Installation	Unit
Qt	130	150	BFPD
Q0	14	16	BOPD

Table 7. Pressure Data

Parameters	Before	After	Unit
Ps	198	198	Psi
Pwf	169	179	Psi

3.5.1. Evaluation of PI (Productivity Index) Before and after Gravel Pack installation

PI (Productivity Index) is a value that expresses the ability of a well to produce. To calculate PI before and after gravel pack installation, the following equation can be used:

PI Before $= \frac{Qt}{Ps-Pwf}$
$= \frac{130}{198-169}$
= 4,4 bbl/psi

PI After $= \frac{Qt}{Ps-Pwf}$
$= \frac{150}{198-179}$
= 7,8 bbl/psi

3.5.2. Evaluation of IPR (Inflow Performance Relationship) Curve Before and After Gravel Pack Installation

The IPR curve is a curve that describes the ability of a formation to produce, by relating well pressure (Pwf) to production rate (Q).

A. Before Gravel Pack Installation

1. Before Determining Qmax

$$Q\ max = \frac{Qt}{1-0.2\left(\frac{Pwf}{Ps}\right)-0.8\left(\frac{Pwf}{Ps}\right)^2} = \frac{130}{1-0.2\left(\frac{169}{198}\right)-0.8\left(\frac{169}{198}\right)^2} = 527{,}4372 \text{ bpd}$$

2. Assume the Pwf and Q values before installing the gravel pack to get an IPR image
   - Calculating the Q value before gravel pack installation at Pwf assumption =190

$$Q = q\ max\left\{1-0{,}2\left(\frac{Pwf}{Ps}\right)-0{,}8\left(\frac{Pwf}{Ps}\right)^2\right\} = 527{,}4372\left\{1-0{,}2\left(\frac{190}{198}\right)-0{,}8\left(\frac{190}{198}\right)^2\right\} = 37{,}67024 \text{ bpd}$$

Table 8. Assumed Value of Pwf and Q Before Gravel Pack Installation

Pwf, psi	Q, bpd
198	0
190	37,67024
160	166,6639
100	366,5315
50	473,8916
0	527,4372

B. After Gravel Pack Installation

1. After Determining Qmax

$$Qmax = \frac{Qt}{1-0.2\left(\frac{Pwf}{Ps}\right)-0.8\left(\frac{Pwf}{Ps}\right)^2} = \frac{150}{1-0.2\left(\frac{179}{198}\right)-0.8\left(\frac{179}{198}\right)^2} = 907{,}108 \text{ bpd}$$

2. Assumptions Pwf and Q values After installation of gravel pack to get IPR curve
   - Calculating the q value after gravel pack installation at Pwf assumption = 190

$$Q = q\ max\left\{1-0{,}2\left(\frac{Pwf}{Ps}\right)-0{,}8\left(\frac{Pwf}{Ps}\right)^2\right\} = 907{,}108\left\{1-0{,}2\left(\frac{190}{198}\right)-0{,}8\left(\frac{198}{190}\right)^2\right\} = 64{,}78682 \text{ bpd}$$

Table 9. Assumed values of Pwf and Q after Gravel Pack Installation

Pwf, psi	Q, bpd
198	0
190	64,7868
160	286,635
100	630,376
50	815,018
0	907,106

To determine the gravity of the IPR curve, plot the Pwf and q data pairs before and after gravel pack installation, thus forming the IPR curve.

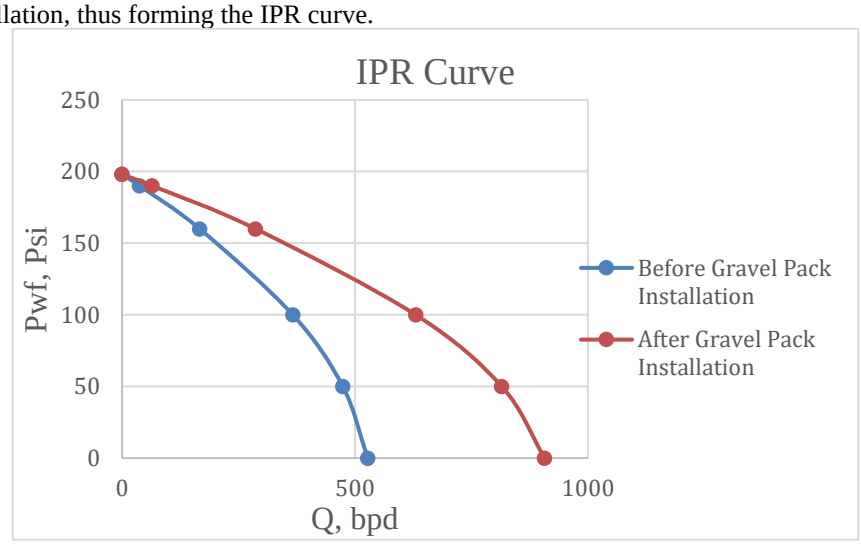

Figure 2. Before and After Gravel Pack Installation

From the results of the production performance analysis above, the production rate is obtained before and after the installation of gravel packs. Where after the installation of gravel pack the production rate has increased. So that this gravel pack installation activity is said to be successful.

3.6. Comparison of Gravel Pack and Screen Liner Methods in Terms of Cost Benefit Analysis

Cost benefit analysis (benefit cost analysis) is an analysis that is very commonly used to evaluate government and private projects. This analysis is a practical way to assess the benefits of a project, this requires a long and extensive review. In other words, analysis and evaluation is needed from various points of view that are relevant to the costs and benefits contributed.

The cost benefit analysis method applied in this study is an analysis that aims to compare the costs that have been invested in the development of the sales system with the benefits or profits obtained by Kalrez Petroleum (Seram) Ltd.

Table 10. Estimation of Cost Benefit Analysis of Gravel Pack and Screen Liner Methods

Methods	Benefit Annual Equivalent US$	Cost Annual Equivalent US$	Ratio
Gravel Pack	1.486.309,077	716.824,8933	2,073461861
Screen Liner	1.300.520,443	545.301,1153	2,38495834

From the table above, the formula for determining equivalent benefits and equivalent costs is

- Benefit Equivalent

  AEB = Σ (Bt/ (1+r)^t)

  AEB : Benefit Equivalent

  Bt : Benefit at Year-t

  r : Discount rate or interest rate

  t : Year

- Equivalent Cost

  AEC = Σ (Ct/ (1+r)^t)

  AEC : Annual Cost Equivalen

  Ct : Cost in year-t
  r : iscount rate or interest rate
  t : Year

From **Table 10**, the first thing to do is to compare the screen liner method with the 0 or "Do Nothing" method. The increase in benefit from method 0 to the screen liner method is 1,300,520.443 and the increase in cost is 545,301.1153. Thus the B/C ratio of the increase is

$$B/C_{S-0} = \frac{\text{Screen Liner Benefit Equivalent}}{\text{Screen Liner Cost Equivalent}}$$

$$B/C_{S-0} = \frac{1.300.520,443}{545.301,1153} = 2,38495834 \text{ US\$}$$

B/C S-0 > 1, then the screen liner method is chosen, then the screen liner method is compared with the gravel pack method, so that the B/C ratio increases as follows:

$$B/C_{G-S} = \frac{\text{Benefit equivalen Gravel Pack} - \text{Benefit equivalen Screen liner}}{\text{Cost Equivalen Gravel Pack} - \text{Cost Equivalen Screen Liner}}$$

$$B/C_{G-S} = \frac{1486309,077 - 1300520,443}{716824,8933 - 545301,1153} = 1,083165472 \text{ US\$}$$

From the results of the above calculations it can be concluded that the screen liner method is better than the gravel pack method, so the US & method is more useful and efficient. In summary, the selection of the above methods can be shown in the table below.

Table 11. Method Selection

Method	Δ Annual Benefits US $	Δ Annual Cost US $	Δ Ratio	Decision
S-0	1300520,443	545301,1153	2,38495834	Screen Liner
G-S	185788,634	171523,778	1,083165472	Screen Liner

IV. CONCLUSION

Based on the results of the above research, the conclusions that can be drawn are as follows:

1. The production of sand to the surface together with fluid is one of the problems that often occurs in the Kalrez Petroleum (Seram) Ltd field such as in the X well. This well uses an artificial lift method using a sucker rod pump. Where this pump is less than optimum for handling sand problems. With the condition of the well like this so that to handle the problem of sandy needs special handling, namely by using the gravel pack method so that the sandy problem can be handled.
2. Based on the smallest sand grain size of 0,024 inch, the size of the gravel pack used in the X well of the Kalrez Petroleum (Seram) Ltd field is 16/30 U.S MESH.
3. Based on the production performance before the installation of gravel pack, the fluid flow rate (Qt) was 130 bfpd, the oil flow rate was 14 bopd, and Q max was 527,4372 bpd. While the results of after the installation of gravel pack the fluid flow rate (Qt) was 150 bfpd, the oil flow rate was 16 bopd, and Qmax was 907,108 bpd. So that the gravel pack installation activity is said to be successful because the flow rate before and after the installation of gravel pack has increased.
4. Based on calculations using cost benefit analysis between the gravel pack and screen liner methods. the screen liner method can be an alternative to overcome the problem of sandiness, this is because it is seen from the value of the B/C ratio > 1 or 2,3. This means that for every one dollar invested in the method, a savings ratio of 2,3 will be obtained. So the screen liner method is more useful and also efficient.

REFERENCES

Araki, N. (2018). Quantitative Analysis Of The Effect Of Perforation Interaction On Sand Production Using The Finite Element Method. Texas: Texas A&M University.

Bergkvam, R. (2015). Parametric Sensitivity Studies Of Gravel Packing. Stavenger. Universitet Stavenger.

Hisham, F. B. (2015). A Critical Review on Roat Cause Analysis on Gravel Packing Design and Installation Issues. Bandar Seri Iskandar. Universitas Teknologi Petronas.

Isehunwa, S., & Farotade, A. (2010). Sand Failure Mechanism and Sanding Parameters in Niger Delta Oil Reservoir. International Journal Of Sience and Technology, 777-782.

Ikporo, B., & Sylvester, O. (2015). Effect of Sand invasion on Oil Well Production. A Case Study of Garon Field in the Niger Delta. International Journal of Engineering Science and Technology, 777-782.

Jamil, N.F. (2011). Production Enhancement From Sand Control Management. Perak: Universiti Teknologi Petronas.

Kamechi, E., & Reise, E. (2015). Sand Production Prediction Using Ratio Of Shear Modulus TO Bulk Compressibility (Case study). Egyptian Journal Of Petroleum.

Mayokun, A. O. (2011). Partical Approach To Effective Sand Prediction, Control And Management Abuja: African University Of Sience and Technology.

Roslan, M. R., Deris, M. N., Hfiz, M., Saebi, S., Afendy, M. N., & Munoz, I. (2010). Rigless Thrpogh-Tubing Gravel Pack For Sand Control in Malaysia. World Oil.

Tananykin, D., & Saychenko, L. (2017). Sand Control Methods For The Development Of Oil & Gas Fields With Hard to Recover Reserves. Revista Expacions.

JOURNAL OF PETROLEUM AND GEOTHERMAL TECHNOLOGY
ISSN: 2723-0988, e-ISSN: 2723-1496
Vol. 5 No. 1 2024

The Selection of Optimal Gas Production Rate using Dynamic Reservoir Simulation in M-Alpha Field

Rahmad Laksamana Pratama [1*], Gerry Sasanti Nirmala[1], Edi Untoro[1], Jatmianto Jayeng Sugiantoro[1], Muhammad Ghazian R.A[1]
[3] Akamigas Energy and Mineral Polytechnic
* corresponding email: rahmadpratama1967@gmail.com

ABSTRACT

The Indonesian government has targeted a gas production rate of 12 BSCFD by 2030 to balance the energy demands and the carbon emission reduction. To achieve this goal, a comprehensive evaluation of a gas field will be carried out regarding the Recovery Factor, Stable Production Period (Plateau Time), Total Production Period, and Profits using a simulation program. Dynamic Reservoir Simulation is an integrated field development simulation that combines physics, mathematics, reservoir engineering, and computer programming to analyze and predict the well's performance under various operating conditions. There are stages in the simulation including Reservoir Model Creation, Initialization, History Matching, and Production Performance Forecasting. This research is a continuation of static reservoir modeling research that was done by LEMIGAS, which was started by reinitializing the model and ended by forecasting the production performance of the M-Alpha field using several gas production flowrate scenarios to find out the optimum gas production rate in ten years period. The simulation result showed that the best production flow rate for ten years is 3 MMSCFD. It gives 78,505% recovery factors, with a cumulative profit of $40,915,872 over a plateau period of 6.6 years.
Keywords: gas production rate, dynamic reservoir simulation, recovery factors, plateau time

I. INTRODUCTION

To strike the balance between energy needs and achieve carbon emission reduction targets, the clean energy transition from hydrocarbon to gas or other energy resources needs to be improved. Therefore, the Indonesian government has targeted natural gas production of 12 BSCFD by 2030 to maintain energy sustainability (Directorate General of Oil and Gas, 2022). To achieve this goal, an integrated field development plan is needed to optimize the gas rate production. M-Alpha field is a greenfield with a condensate gas type reservoir, located in the North Kalimantan Region as a part of the Bulungan Delta. A field development scenario will be carried out to increase production in the M-Alpha field. Therefore, an evaluation is needed regarding the appropriate injection rate, constant gas production time (plateau time), and calculation of the optimum profit.

There are many methods of field production forecasting and project planning by these results. One of the methods used to make field development planning is by Reservoir Simulation. It is a complement to field observations, experiments, laboratory tests, well tests, and an analytic model, and used by reservoir engineers to investigate the displacement of processes, to compare and contrast the characteristics of different production scenarios, or as a part of inverse modeling to calibrate reservoir parameters by integrating static and dynamic (production) data (Sankaran et al, 2020; Tan et al, 2022; Zargar & Thakur, 2022). Reservoir simulation combines physics, mathematics, reservoir engineering, and computer programming to develop a tool (in this case a model) to analyze and predict the performance or how fluid flows through reservoir rocks to the surface over time under a wide variety of operating conditions. These results are then used to optimize field development plans to analyze the operational and to decide the investment decisions (Ertekin et al., 2001; Lie, 2019).

The two most common types of reservoir models are Black Oil models and composition models (Ahmed, 2019). The Black Oil model assumes that the saturated phase properties of the two hydrocarbon phases (oil and gas) depend only on pressure. Composition models also assume two hydrocarbon phases, allowing the definition of many hydrocarbon components (Fanchi, 2006). According to (Chen, 2007), the gas component of the Black oil model is divided into two parts, one part is in the gas phase known as free gas, and the other part is in the oil phase known as solution gas. Free gas is characterized by the density ρ_g, but solution gas has its density (Chen, 2007). In this research, we try to characterize the M-Alpha field reservoir type and choose the optimum production scenario. This is a development of previous research that produced a Static Reservoir Model in the M-Alpha field and simulations at an early stage.

II. METHODS

2.1. Equipment and Materials

The data used in this study was previous data from previous research and laboratory tests carried out by BBPMGB "LEMIGAS". The data include Fluid Composition Analysis, Routine Core Analysis, Rapid Formation Test (RFT), Well

Test, and Reserves Analysis. Well X-1 is a producing well in the M-Alpha field which is used as an object in this research with fluid composition as shown in **Table 1.**

Table 1. M-Alpha field Reservoir Fluid Composition

Component	ZI	Weight fraction	MW	SG (Gram/cc)
CO2	2.97	5.6745	44.01	0.777008
N2	0.1	0.12161	28.013	0.803999
C1	79.9	55.648	16.043	0.425002
C2	5.94	7.7542	30.07	0.548008
C3	5.39	10.318	44.097	0.581999
IC4	1.27	3.2046	58.124	0.556994
NC4	1.37	3.457	58.124	0.579003
IC5	0.59	1.848	72.151	0.619995
NC5	0.33	1.0336	72.151	0.626002
C6	0.42	1.5316	84	0.684998
C7+	1.72	9.4084	126	0.763

The data was analyzed using software such as ®ECLIPSE PVTi, ®PROSPER, Microsoft Excel, and ®PETREL RE. Software Eclipse PVTi was used to obtain a phase diagram model of M-Alpha field reservoir fluids. Meanwhile, an Inflow Performance Relationship (IPR) graph was obtained using PROSPER, and PETREL was used to perform dynamic reservoir modeling and production forecasting in several different production scenarios. To analyze the data, a computer with high specifications is needed. To perform this study, we were using a laptop unit with specifications of AMD Ryzen 7 4800H processor (~2.9 GHz), Memory Capacity RAM 16 GB, SSD Storage Capacity 500 GB, VGA NVIDIA Geoforce GTX 1650Ti, and *Display Monitor* 1920 x 1080 px.

2.2. Research Methodology

Using several gas production flow rate scenarios, an optimum gas production flow rate was determined. The parameters used to determine the optimum conditions include the Recovery Factor, Stable Production Period (Plateau Time), Total Production Period, and economic elements. The stages of research carried out include Data Analysis, Property Modelling, Initialization, History Matching, and Forecasting. Data analysis was done to obtain the data needed to start a dynamic reservoir simulation. These data were Phase Diagrams and PVT data models. In this case, the PVT data models were based on Constant Composition Expansion and Constant Volume Depletion test results using the PVTi program in Eclipse software. The test was done by applying Peng-Robinson 3-parameter equation of state and Lohrenz-Bray-Clark viscosity correlation, Permeability Distribution Equation (using power regression analysis), IPR and VLP (using PROSPER software with Multirate C and n IPR equations), Datum Depth (Fluid contact, in this case GWC) and Pressure Distribution Equation (using linear regression analysis). The Inflow Performance Relationship (IPR) graph was obtained from equation (1), as follows:

$$Q_g = C(p_r^2 - p_{wf}^2)^n \quad (1)$$

For natural gas production, the estimated maximum production of each well was determined by test data and does not exceed 30% AOF of the IPR curve (PTK 037, 2017; PTK 037, 2021).

The next stage was Property Modelling, where the properties of the reservoir will be put into a static reservoir model before doing the actual simulation. In this case, the reservoir model has been made by BBPMGB "LEMIGAS". Several types of data represent the actual condition of the reservoir such as Geometric Data (grid cell size, volume, elevation, slope, etc.), structural and stratigraphic data, Petrophysical Data, Reservoir Fluid (PVT) Data, Well and Production History, etc. Data can be derived from log or laboratory data that is input as a scale-up from log data.

The Initialization process was carried out to equalize the reserve volume (hydrocarbon in place) from the results of volumetric calculations and simulation results. The volumetric method can be used when the available data is incomplete (Ardiansyah et al, 2021). It is useful for determining the value of the initial hydrocarbon in place, ultimate recovery, and recovery factor. Due to limited laboratory test data to complete the required data, several equations have been provided on PETREL according to the type of formation, in this case, *consolidated sandstone* was selected as the formation type. The equations include Corey correlation to find the value of relative permeability to fluid saturation, and Newman correlation to find the compaction value of rocks.

Then History Matching was conducted to see the difference and to match data between the observed data (pressure and production) and the simulation results. This was done to ensure that the input data was correct and adequate to start the simulation. The smaller the difference between the simulation results and the actual data, the more accurate the model's ability to simulate reservoirs. Thus, the more reliable the simulation result. The acceptable difference for in-place volume is < 5% (Pamungkas, 2011). The last stage was the Forecasting process which was carried out with specific parameters according to the goals of the simulation or field development scenario that had been planned.

Each field has its characteristics which may affect the decision-making of optimum field development plan. A good data analysis will provide accuracy and predictability in production forecasting of the project outcome to committing the financial risk associated with the project and ensuring the correct production action (Tan et al., 2022). In the oil and gas industry, data analytics plays an important role in reducing the risk inherent in the development of subsurface resources by reducing operational cost, improving efficiency, and increasing the production and reservoir recovery together with good quality field data (log, fluid, core, etc.) to ensure the low uncertainty (Sankaran et al., 2020). This research was conducted by forecasting the production of the M-Alpha field for the next ten years starting from 24th May 2022. The evaluation includes the economic element of the final profit obtained over the past ten years where operating costs are negligible.

III. RESULTS AND DISCUSSION

3.1. Production Performance

Generally, if the reservoir temperature (T) is above the critical temperature (T_c) of the hydrocarbon system, then the reservoir is classified as a natural gas reservoir. According to the phase diagram, natural gas can be classified into four categories, namely Retrograde Gas Condensate Reservoir, Near Critical Gas Condensate Reservoir, Wet Gas Reservoir, and Dry Gas Reservoir (Ahmed, 2019). Using ECLIPSE PVTi, a phase diagram model of the M-Alpha field reservoir was obtained, as can be seen in **Figure 1** and **Table 2.**

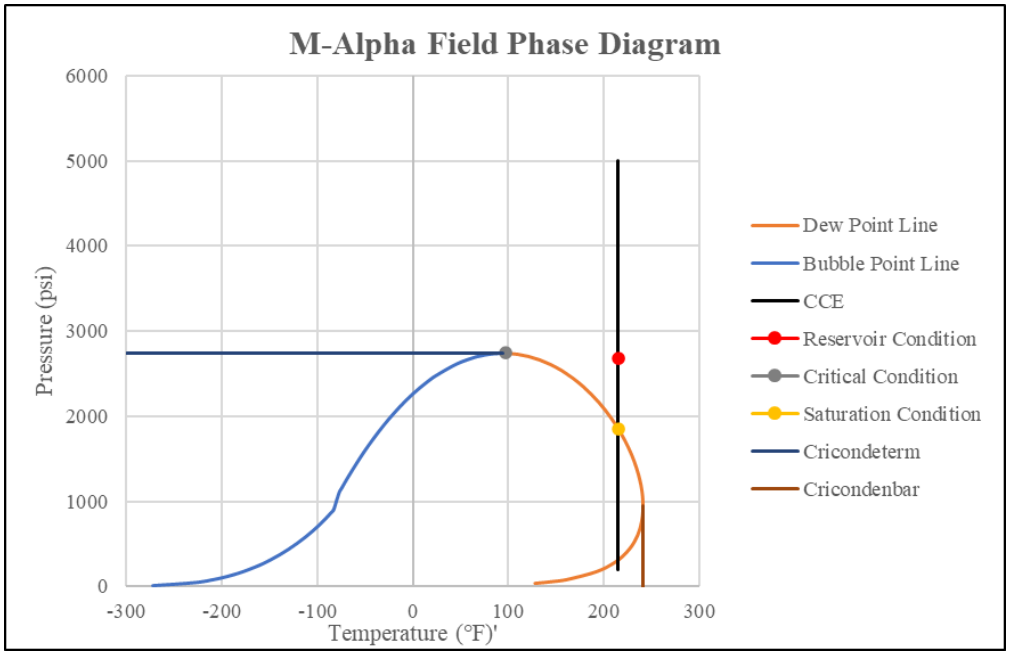

Figure 1. Phase Diagram of Reservoir X

Table 2. Fluid Properties of Phase Diagram and PVT Modeling Using Eclipse PVTi

Condition	Pressure	Temperature
	psi	°F
Critical Point	2751.56	97.67
Reservoir	2676.47	214.8
Saturation	1847	214.8

In **Figure 1,** the blue dot on the top of the bubble point line represents the critical condition, the green dot represents the saturation condition, and the orange dot represents the reservoir conditions. PVT data was also obtained through Constant Composition Expansion (CCE) and Constant Volume Depletion (CVD) test modeling. GOR and condensate density values were obtained from well test data respectively 32633 SCF and 62.5°API. Based on these results, it can be said that the M-Alpha field is a condensate gas reservoir. This is convenient with the (Ahmed, 2019) theory which states that condensate gas reservoirs are characterized by the temperature of the reservoir lying between the critical temperature and cricondeterm, GOR from 8000 to 70000 scf/stb, and condensate density > 50°API. Meanwhile, from PVT data, it is known that the Gas Formation Volume Factor (Bg) at reservoir conditions is 0.006050 cuft/SCF.

The relationship between porosity and permeability data was obtained from Core Analysis and Well Test with Power Regression Analysis. **Figure 2** depicts the distribution of the effective porosity in the reservoir. The distribution of effective porosity appears to be in line with the formation types that have been modeled previously, where the purple color depicts shale formations with very small porosity and the other colors depict sandstone formations with varying porosity, with the largest porosity value being 21.86%. Color variations indicate the level of porosity, where the closer to red, the greater the porosity, and the closer to purple, the smaller the porosity. An equation is obtained which describes the distribution of permeability values in the reservoir, as follows:

$$k\ (md) = 2.18.10^{6} \times \Phi^{6.2258} \quad (2)$$

From equation (2), the permeability value can be determined, which was 160.285 md.

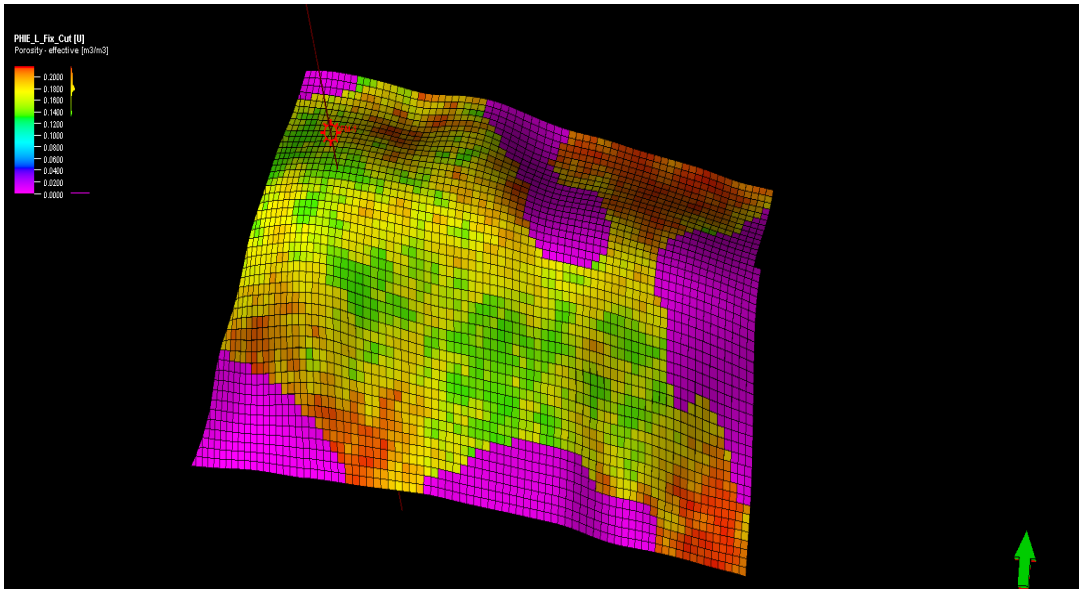

Figure 2. The distribution of the effective porosity in the reservoir

Using PROSPER software, an *Inflow Performance Relationship* (IPR) graph was obtained from the production of Well X-1. The well-testing method used was *the Drill Stem Test* (DST) with a tubing size of 2,992 inches. It was carried out in several stages with different flow rates, so it produced several *Vertical Lift Performance*s (VLP) with different *Tubing Head Pressure* (THP) as shown in **Figure 3**. The green line is the IPR and the red lines are the VLPs. The blue dots represent the intersection point between IPR and VLP with a combination of gas rate and bottom hole pressure. The maximum gas rate, which is also called AOF, is shown in **Figure 2** at 68,227 MMSCFD. Using the assumption that the optimum production limit is ≤ 30% AOF, then the optimum production limit for well X-1 is less than 20,468 MMSCFD. This is by intersection point 6. In addition, we get a C value of 0.12195 MMSCFD/psi^2 and an n value of 0.83796.

The analysis of the *Rapid Formation Test* (RFT) on Well X using linear regression analysis showed that the contact between the aqueous and gas phases occurred at a depth of 6500 ft or 1981.1 meters. The pressure gradient was 0.1456 psi/ft for gas and 0.453 psi/ft for water, respectively. The regression equation describes the pressure distribution that applies in field reservoir X, as follows.

$$P, psi = 0.453(d, ft) - 226.86 \quad (3)$$

for water-bearing formation, and

$$P, psi = 0.1456(d, ft) - 1770.8 \quad (4)$$

for gas-bearing formation.

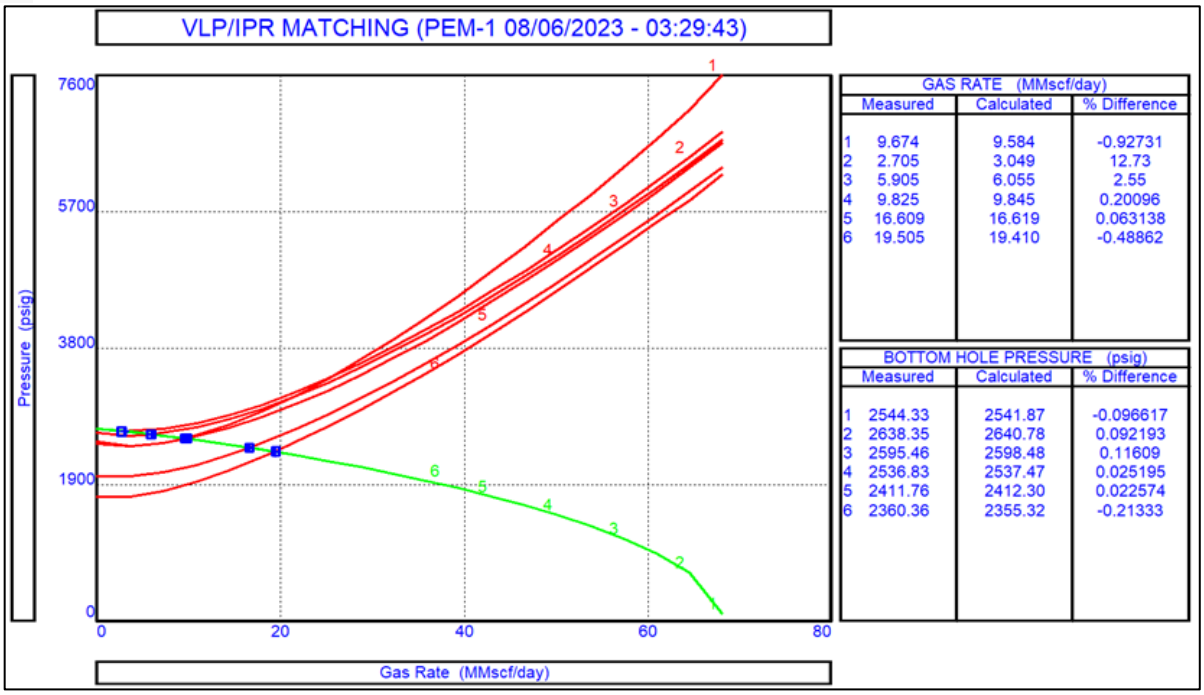

Figure 3. The IPR and VLP matching

3.2. Initialization and History Matching

The initialization process is carried out on the well reservoir model, with the previous configuration. The Initial Gas in Place (IGIP) for the M-Alpha field reservoir using volumetric calculation showed a result of 9610 MMSCF but the simulation result was 20277.24 MMSCF. The difference between IGIP from volumetric and simulation was 71.38%. This significant difference resulted because the area used for simulation are whole reserves area or 3P area (Proven (P1) + Probable (P2) + Possible (P3)). Meanwhile, the area used for volumetric IGIP calculation is 2P area (Proven (P1) + Probable (P2)). After adjusting the area for simulation, the second attempt of initialization resulted in IGIP 9539.666 MMSCF, minimizing the difference significantly up to 0.73 %. As the difference is < 5% (difference tolerance), the initialization process was considered successful.

After initialization, an alignment process was carried out on Well X-1, sequentially this alignment was carried out on Bottom Hole Pressure, Tubing Head Pressure, Gas Production, and Condensate Production. The result of the history-matching process can be seen in **Figure 4**. There is a discrepancy in the condensate production data, due to several factors, including limited data (SCAL and PVT data) and very low liquid saturation. After matching various VLP data with different THPs, the observed data and simulation result match with VLP data of 1966.99 psi THP, and a flow rate of 9,825 MMSCFD. This flow rate will be used as the maximum flowrate parameter in the dynamic simulation.

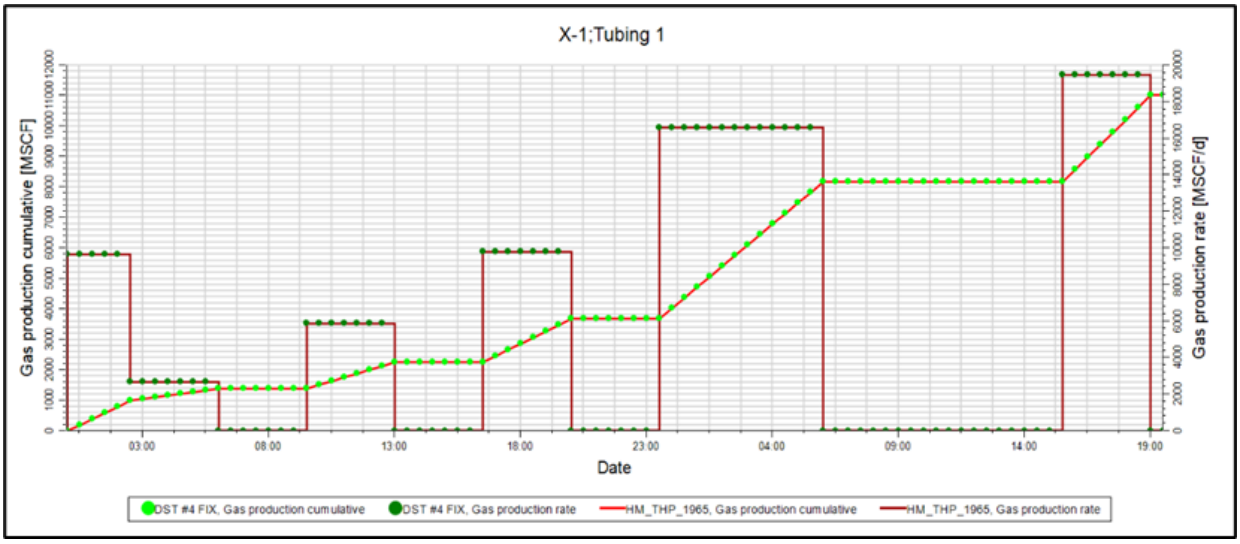

Figure 4. The result of the Initialization and History Matching process

3.3. Production Forecasting

In this stage, sensitivity analysis was used in gas production flowrate. The initial gas flow rate was maintained at 9,825 MMSCFD and a plateau period of around 1.69 years started from the initial simulation. Then proceed with sensitivity for the production flowrate to find out the most profitable production scenario in the 6 years, with a maximum THP of 100 psi and a minimum gas flowrate of 1000 MSCFD. In this scenario, the profits obtained during the production period were also calculated. The calculation was based on presidential decree No. 121, 2020, which states that the highest natural gas price in the domestic market (Indonesia) is USD 6/MMBTU (The Amendments to Presidential Regulation Number 40 of 2016 concerning Determination of Natural Gas Prices, 2020). The plot of gas production rate versus time was presented in **Figure 5** and the results of the sensitivity analysis, plateau time, and profits were presented in **Table 3**.

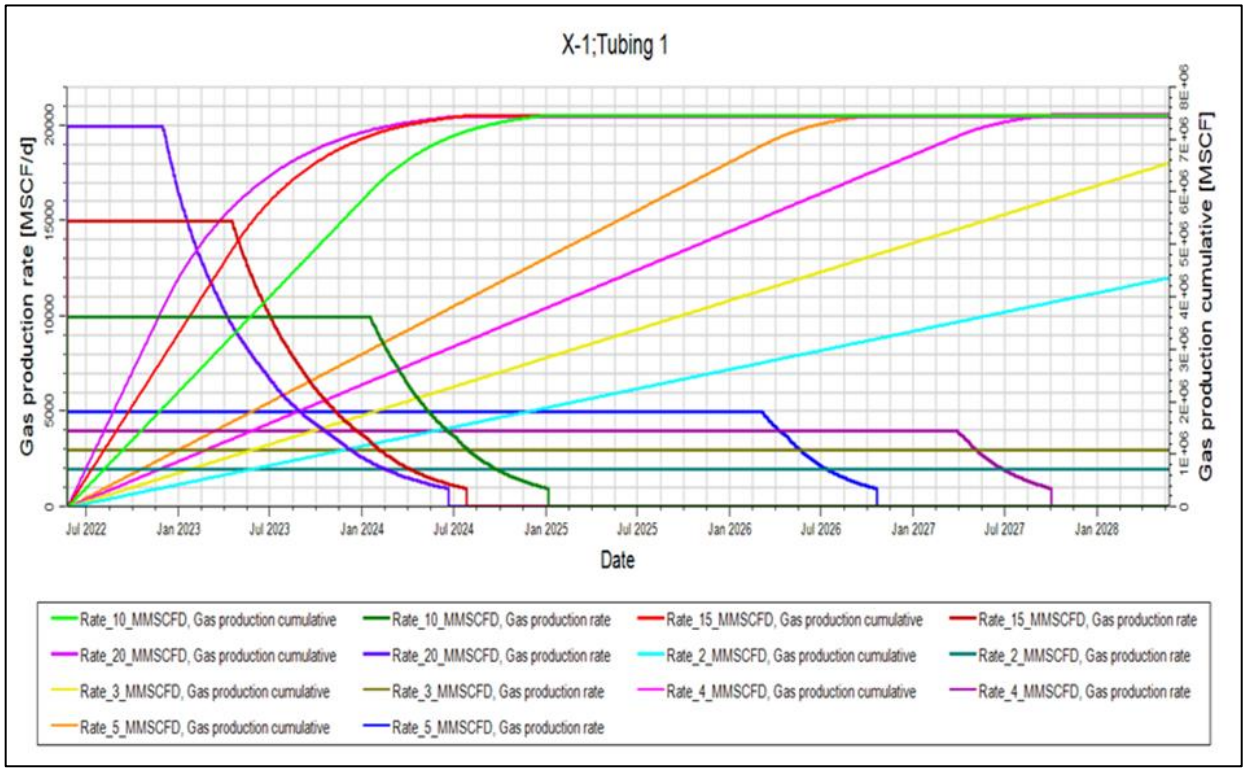

Figure 5. The Simulation Results of Flow Rate and Cumulative Gas Production from 2022 – 2028

Table 3. Forecasting and Economic Analysis of M-Alpha Field with Variation of Gas Production Rate Scenarios

Flowrate Scenario		RF	Plateau	Plateau	Production	Prod. Time	Profit/day	Cumulative Profit
No	MMSCFD	%	End	Year	End	Year	$	$
1	20	78.054	01/12/2022	0.5	23/06/2024	2.1	124,440	23,768,040
2	15	78.300	17/04/2023	0.9	27/07/2024	2.2	93,330	30,612,240
3	10	78.419	18/01/2024	1.7	06/01/2025	2.6	62,220	37,580,880
4	5	78.488	07/03/2026	3.8	21/10/2026	4.4	31,110	43,025,130
5	4	78.496	30/03/2027	4.9	05/10/2027	5.4	24,888	44,076,648
6	3	78.505	Ongoing	6.6	Ongoing	7.0	18,666	40,915,872
7	2	78.524	Ongoing	10.0	Ongoing	10.0	12,444	27,277,248

As the result above, the observed parameter (Recovery Factor (RF), Plateau time, Production Lifetime, and Profit), seems to have increased as the wells started to produce. There was an exception on Scenario 6 and 7 because the production was forecasted to still be ongoing after a year. The parameter enhancement from one scenario to another was varied. The RF and Profit kept declining as the gas rate decreased. As an illustration in **Figure 5**, from scenarios 1 to 2 the increase of RF was 0.315% and the profit was 28.8%. In the end, the enhancement from scenarios 5 to 6 was 0.011% for RF and 2.06% for profit. This change was very minuscule compared to the enhancement at the beginning. However, in the case

of a period of plateau and production time, the enhancement becomes more varied. The increase from certain scenarios was more substantial than others. For example, the plateau year from scenario 2 increased by 0.4 years or about 71.73% from scenario 1. A drastic change occurred in scenario 4 when the plateau year increased more than two-fold from the previous scenario (scenario 3) and gained extra after 2.1 years. Then, the enhancement became smaller but a sudden increase occurred again in scenario 7 when the plateau year was increased by 3.4 years or about 51.58% from scenario 6. Fulfilling the ten years and prediction was still ongoing.

According to simulation using scenario 7, where the plateau and production time have not yet reached the end time, the M-Alpha field potentially can be operated over ten years. From this point of view, it can be inferred that Scenario 7 was more advantageous than other scenarios. Moreover, it gave the best recovery factor which was 78.524%. However, if the total gross profit obtained from gas sales was also taken into account, the enhancement was not too significant (around 1.05%) compared to scenario 6. If the payback period for developing the M-Alpha field and the profits were considered, then scenario 6 was more profitable because the payback period is faster than scenario 7. Taking other factors into account, scenario 6 appears to be the best option for gas production in the M Alpha field. It gave 78.505 % of RF, and even though the RF value is smaller than scenario 7, the difference was small so gas recovery can be said to remain high.

Using several software and calculations, an analysis to determine the best production scenario has been carried out. With a phase diagram model, the M-Alpha field reservoir type was determined and although the porosity value does not exceed 21.86%, the reservoir has a permeability value of 160.285 md which indicates that the reservoir has a good ability to flow fluid. By IPR and VLP matching, then the optimum production limit for well X-1 was determined not more than 20,468 MMSCFD with a maximum flowrate of 9,825 MMSCFD. This value becomes the basic calculation for subsequent production forecasting. Using sensitivity analysis, and considering the economic analysis of the M-Alpha field, the best production flowrate was determined at 3 mmscfd for a maximum of 7 years of production period. Regardless of this potential, gas production rate determination is always following consumer requests that have been approved in the prior business contract between the company and the government.

IV. CONCLUSION

A reservoir simulation analysis was done to select the optimum gas production rate for well X in the M-Alpha field which is located in North Kalimantan. Based on the PVT analysis, the M-Alpha field is a condensate gas reservoir with the GOR 32633 SCF and a density of 62.5°API. The IGIP obtained was 9539,666 MMSCF indicating that this field has very promising productivity. Using sensitivity analysis, the best production scenario was obtained with a gas flowrate of 3 mmscfd. It gives the best recovery factor which is 78.505% with a cumulative profit of $40,915,872 over a plateau period of 6.6 years. The effect of altering the gas production rate is minuscule towards the recovery factor value of the M-Alpha field. Indicated by less than a 1% increase in recovery factor. The decreasing of the gas flowrate gives a more effective lifetime of the field which gives more profit for the benefit. According to the analysis and calculations that have been carried out, it can be concluded that the M-Alpha field has optimum productivity for a maximum of 7 years with a flowrate of 3 mmscfd.

ACKNOWLEDGEMENTS

The results of data analysis in this research were provided by BBPMGB "LEMIGAS" Jakarta, Indonesia during the Student Field Working Program in 2023.

REFERENCES

Directorate General of Oil and Gas. (2022). The Important Role of Natural Gas in the Energy Transition. Jurnal Migas, 9, 22–23.

Sankaran, S., Matringe, S., Sidahmed, M., Saputelli, L., Wen, X.-H., Popa, A., & Dursun, S. (2020). Data Analytics in Reservoir Engineering. Society of Petroleum Engineers. https://doi.org/10.2118/9781613998205

Tan, V., Aziz, K. Ab., & Razavi, S. H. (2022). Data Analytics for Effective Project Management in the Oil and Gas Industry. In A. Asmawi (Ed.), Proceedings of the International Conference on Technology and Innovation Management (ICTIM 2022) (Vol. 228, pp. 233–242). Atlantis Press International BV. https://doi.org/10.2991/978-94-6463-080-0_20

Zargar, Z., & Thakur, G. C. (2022). Importance of reservoir simulation and early reservoir management for successful field development—Case study. Energy Reports, 8, 5038–5052. https://doi.org/10.1016/j.egyr.2022.03.189

Ertekin, T., Abou-Kassem, J. H., & King, G. R. (2001). Basic Applied Reservoir Simulation (Vol. 7). Society of Petroleum Engineers.

Lie, K.-A. (2019). An Introduction to Reservoir Simulation Using MATLAB/GNU Octave: User Guide for the MATLAB Reservoir Simulation Toolbox (MRST). Cambridge University Press. https://doi.org/10.1017/9781108591416

Ahmed, T. H. (2019). Reservoir Engineering Handbook (Fifth edition). Gulf Professional Publishing

Fanchi, John R. (2006) Principles of Applied Reservoir Simulation (Third Edition), Gulf Professional Publishing, Pages 255-281, ISBN 9780750679336, https://doi.org/10.1016/B978-075067933-6/50016-7.

Chen, Z., (2007). *Reservoir Simulation: Mathematical Techniques in Oil Recovery.* Philadelphia: Society for Industrial and Applied Mathematics.

PTK 037/SKKMA0000/2017/S0 Year 2017 Revision 01 concerning Plan of Development (POD)

PTK 037/SKKMA0000/2021/S9 Year 2021 Revision 03 concerning Plan of Development (POD)

Ardiyansyah , M. Triany, N. Setiati, R. Koesmawardan, WT. (2021). Volumetric calculations for estimating reserves of oil and gas energy resources. International Conference on Research Collaboration of Environmental Science. IOP Conf. Series: Earth and Environmental Science 802 (2021) 012047 IOP Publishing doi:10.1088/1755-1315/802/1/012047.

Pamungkas, J. (2011). Pemodelan dan Aplikasi Simulasi Reservoir (1st ed.). Program Studi Teknik Perminyakan UPN "Veteran" Yogyakarta.

The Amendments to Presidential Regulation Number 40 of 2016 (2020) concerning Determination

JOURNAL OF PETROLEUM AND GEOTHERMAL TECHNOLOGY
ISSN: 2723-0988, e-ISSN: 2723-1496
Vol. 5 No. 1 2024

Analysis of Scale Problem using Acidizing Stimulation in Field Z Kalrez Petroleum (Seram) Ltd

Sumina Idrus[1*)]
Oil and Gas Production Engineering, Ambon State Polytechnic
* corresponding email: idrussumina@gmail.com

ABSTRACT

The annual decrease in production at well Z occurs due to scale deposits that impede fluid flow. Scale is a production problem due to the mixing of two types of water with different properties so that the solubility limit of the compound in the formation water is exceeded. To overcome the scale, stimulation is carried out with an acidizing method using a type of acid (HCL 10%). Evaluation was conducted to determine the effect of acidizing stimulation on scale based on productivity index (PI), inflow performance relationship (IPR) curve and comparison of stimulation methods. Evaluation of test results after acidizing stimulation of well Z experienced an increase in production. Productivity Index increased from 4.748 bbl/psi to 9.036 bbl/psi. Based on the IPR curve before acidizing, the maximum flow rate (Q max) = 324,107 bpd, increased to Qmax = 769,021 bpd.
Keywords: *Cost Benefit, Productivity Index, Scale, Acidizing Stimulation*

I. INTRODUCTION

Scale is a production problem in water systems caused by changes in pressure, temperature and pH that cause the ion balance to exceed solubility and form deposits in reservoirs, production zones, or along oil and gas production pipelines. By mixing two different types of water so that the solubility limit of the compound is exceeded in the resulting water mixture and scale deposits are formed (Diky & Syahrial 2017).

Kalrez Petroleum Seram ltd's "Z" well has considerable scale potential that has resulted in a decline in production over the years. In 2017, the indication of scale in the Z well was discovered when conducting well work in the form of unplugging the production circuit. The presence of solids in the reservoir can reduce the permeability of the rock thus reducing oil production. When scale sticks to flow pipes, it damages the pipes and complicates oil and gas production (Diky & Syahrial 2017).

Scale must be monitored continuously because when oil moisture content is low and dispersed water is small, the rate of scale formation is proportional to the rate of free water formation, depending on where the water in the formation becomes saturated. In an effort to restore and maintain the amount of production that has decreased due to scale, a work over operation is carried out. One of the work over jobs is to stimulate acidizing Agusandi, D. P. (2017).

Acidizing stimulation is a well improvement process that aims to increase the flow rate in the formation by injecting a certain amount of acid into the well. The main principle of this method is to dissolve materials that block reservoir flow by injecting acid into the well. Usually, the objective The purpose of acidification is to reduce formation damage and increase permeability by expanding rock pores and dissolving particles that inhibit flow in rock pores (Mety & Rahmact, 2015).

II. METHODS

The methods used in this study include field observations, formation water sampling and then analyzed quantitatively to obtain the data needed in the study.

2.1. Stiff & Davis Method

The Stiff & Davis method is used to determine the potential for calcium carbonate ($CaCO_3$) scale formation. Stiff & Davis have developed a formation water analysis method that can be applied to brine by taking into account the ion strength parameter as a correction to the total salt concentration and temperature (Henk, S., et al., 2022).

The approximate tendency of calcium carbonate scale formation can be determined based on the Scale Index (SI) value with the following conditions:

$$SI = pH - K - pCa - pAlk \quad (1)$$

- If the SI value < 0 (negative), the system is not saturated by $CaCO_3$ and the tendency for scale formation is low.
- If the SI value > 0 (positive), then the system is saturated by $CaCO_3$ and there is a tendency to form scale. If the SI value = 0, then the system is at the saturation point, and scale will not form.

Table 1. Ionic Strength Conversion Factor

Ion	Conversion Factor
Na^+ (Sodium)	2,20 x 10^5
Ca^{2+} (Calcium)	5,00 x 10^5
Mg^{2+} (Magnesium)	8,20 x 10^5
Cl^- (Chloride)	1,40 x 10^5
HCO^{3-} (Bicarbonate)	0,82 x 10^5
$CO3^{2-}$ (Carbon Trioxide)	3,30 x 10^5
$SO4^{2-}$ (Sulfate)	2,10 x 10^5
$HCO3^-$ (Bicarbonate)	-

2.2. Skillman, McDonald & Stiff Method

The Skillman, McDonald & Stiff method was used to determine the tendency of calcium sulfate ($CaSO_4$) scale formation. The determination of $CaSO_4$ scale formation tendency using this method is based on the following equation: The estimation of the tendency of calcium sulfate ($CaSO_4$) scale formation is based on the results of S calculation, by comparing the actual concentrations of Ca^{2+} and SO_4^{2-} present in the formation water with the following conditions:

$$S = 1000 (\sqrt{x^2} - 4k - x) \quad (2)$$

The estimation of the tendency of calcium sulfate ($CaSO_4$) scale formation is based on the results of S calculation, by comparing the actual concentrations of Ca^{2+} and $SO4^{2-}$ present in the formation water with the following conditions:

- If the S value is smaller than both the actual concentrations of Ca^{2+} and $SO4^{2-}$, then it tends to form scale $CaSO_4$.
- If the S value is greater than both the actual concentrations of Ca^{2+} and $SO4^{2-}$, then the water is not saturated with $CaSO_4$ and the $CaSO_4$ scale is not formed.

2.3. Acidizing Method

This method is used to overcome the flow resistance that occurs in the reservoir by dissolving the material through acid injection into the well. The main objective of acidizing is to reduce the effect of permeability reduction (formation damage) that occurs around the wellbore. This is done by expanding rock pores and dissolving particles that inhibit flow in the rock (Mety, A., & Rahmact, S. 2015).

1. Determining the Price of Formation Fracture Pressure
   $BHP_{rekah} = G_f \times D$ (3)

2. Determining the Maximum Acid Injection
   Hydrostatic Pressure = $0{,}05 \times \rho_{acid} \times D$ (4)
   Surface Pressure = BHP_{rekah} – Hydrostatic Pressure (5)

3. Determination of Acid Injection
   $VT = \frac{\text{ID tubing}^2}{1029{,}4} \times \text{Length}$ (6)

4. Annulus Volume
   $VA = \frac{\text{ID Casing}^2}{1029{,}4} \times \text{Length}$ (7)

2.4. Cost Benefit Analysis Method

Cost/Benefit Analysis or CBA is one of the risk evaluation methods that helps users in selecting or determining the action options that need to be taken in dealing with a risk. This approach measures and compares the benefits and costs of various risk action options (Winsky, 2019).

1. Annual Equivalent Benefit
   $AEB = \Sigma(Bt/(1+r)^t)$ ..... (8)

2. Annual Equivalent Cost
   $AEC = \Sigma(Ct/(1+r)^{\wedge}t)$ .....(9)

III. RESULTS AND DISCUSSION

3.1. Formation Water Analysis

Scale formation in general is always related to formation water, so the characteristics of formation water must be known. The formation water data obtained in this study came from the analysis of Geoservices Laboratories Kalrez Petroleum (Seram) LTD.

Table 2. Formation water test samples

No	Parameters	Unit	Analysis Result
1.	Cations		
	Na^+	mg/I	9216
	Ca^{2+}	mg/I	119,9
	Mg^{2+}	mg/I	383.3
	Ba^{2+}	mg/I	4.6
	Fe^{3+}	mg/I	0.36
2	Anions		
	Cl^-	mg/I	14070
	SO_4^{2-}	mg/I	11
	CO_3^{2-}	mg/I	Nill
	HCO_3^-	mg/I	2521
3	TDS (calc)		26326,16
	H2S	mg/I	5,4

Table 3. Results of Formation Water Analysis

Component	Result mg/I	Conversion Factor	Ionic Strength
HCO_3^-	2521	$0{,}82\times10^{-5}$	0,0206722
CI^-	14070	$1{,}40\times10^{-5}$	0,19698
Ca^{2+}	119,9	$5{,}00\times10^{-5}$	0,005995
Mg^{2+}	383,3	$8{,}20\times10^{-5}$	0,031431
$SO4^{2-}$	11	$2{,}10\times10^{-5}$	0,000231
Na^+	9216	$2{,}20\times10^{-5}$	0,202752
Total Ionic Strength			0,4581

To determine the tendency of the formation of scale $CaCo_3$ and scale $BaSo_4$ in well Z, namely by calculating the value of scaling index (SI) and solubility of gypsum (S), using stiff & davis and Skillman, McDonald & Stiff methods. The first step that must be done is to determine the ionic strength value of each ion by multiplying the ion concentration with its conversion factor so that it will get the ionic strength results as in **Table 3.**

After getting the results of ionic strenght, continue to determine the value of the scaling index (SI) and solubility of gypsum (S) by entering the value in equations 1 and 2. The results of the SI value = 8.34 are positive, so in the Z well formed scale $CaCO_3$, solubility of gypsum S = 0.01 the value of S is smaller than the two actual concentrations of Ca^{2+} and $SO4^{2-}$, then it tends to form scale $CaSO_4$.

3.2. Acidizing Stimulation

To overcome scale and maintain production rates, acidizing stimulation is carried out by injecting acid so that the scale can be dissolved.

Table 4. Well Z data

Parameters	Inch	Meters	Feet
Perforation length (open hole)		16,8	55
Wellbore diameter (initial)	2 3/8		0,19792
Scale thickness estimation	1		0,08333
Wellbore diameter (scale)	2 7/8		0,23958

The type of acid used to treat scale in the Z well of Kalrez Petroleum (seram) Ltd is 10% hydrochloric acid (HCL 10%). The formation fracturing pressure gradient is calculated to find out how much pressure i s needed in the acid injection process so that no fractures occur in the formation BHP_{rekah} = 91 psi. Next calculate the hydrostatic pressure and surface pressure in order to know the maximum rate of acid to be injected hydrostatic pressure = 54 psi and Surface pressure = 37 psi. The next step is to calculate the volume of acid to be injected so that the scale that inhibits perforation can be dissolved Vol. Displacement = 63 bbl.

a. Injectivity Test

Injectivity test was conducted by injecting 150bbl of water and chemical mixture into the well to clean the well and as an initial stage to estimate the injection rate that will be used t o pump acid so that the acid injected into the formation pressure does not exceed the formation fracturing pressure.

b. Mixing

The mixing process is basically making and processing a mixture of acids added with acid chemicals to make it suitable for scale countermeasures.

c. Preflush

Preflush aims to clean the oil in the perforation hole, because if HCL meets oil it will form clumps.

d. Acidizing Stimulation Design

The selection of the type of acid and additive used must be adjusted to the type of rock and formation damage in an oil and gas well. Before performing acidizing stimulation, it is necessary to know the design and calculation data required. The goal is to know some important parameters so that the implementation in the field runs as planned.

3.3. Evaluation of the Success of Acidizing Stimulation

3.3.1. Based on Productivity Index (PI)

Productivity Index (PI) expresses the ability of a productive formation to flow fluid to the bottom of the well at a certain drowdwon price. Acidizing stimulation is said to be successful if there is an increase in PI.

Table 5. Well Z data

Parameters	Inch	Meters	Feet
Perforation length (open hole)		16,8	55
Wellbore diameter (initial)	2 3/8		0,19792
Scale thickness estimation	1		0,08333
Wellbore diameter (scale)	2 7/8		0,23958

- PI Before Acidizing Stimulation

$$PI = \left[\frac{Q}{Ps - Pwf}\right]$$

$$= \left[\frac{89}{147,04 - 121,294}\right]$$

= 4,748 bbl/psi

- PI After Acidizing Stimulation

$$PI = \left[\frac{Q}{Ps - Pwf}\right]$$

$$= \left[\frac{120}{147,04 - 133,76}\right]$$

= 9,036 bbl/psi

3.3.2. Evaluation Based on Inflow Performance Relationship (IPR) Curve

Inflow Performance Relationship (IPR) curve is a plot between well bottom flow pressure (Pwf) and production rate (Q). In the Z well of Kalrez Petroleum Seram Ltd, the IPR curve was made using the Vogel method, because this method has good accuracy for two-phase flow.

Table 6. Assumed values of Pwf and Q before acidizing stimulation

Pwf (psi)	Q (bpd)
147.04	0
140	64.125
112	160.098
84	223.689
56	272.084
28	318.499
0	324.107

Table 7. Assumed values of Pwf and Q after acidizing stimulation

Pwf (psi)	Q (bpd)
147.04	0
140	152.153
112	379.872
84	530.512
56	645.584
28	725.087
0	769.021

To determine the Inflow Performance Relationship (IPR) curve, plot the graph of the Pwf assumption with the Q value before and after acidizing stimulation to see the comparison of acidizing stimulation. The results of the IPR curve before and after acidizing can be seen in **Figure 1.**

3.4. Comparison of 10% Hydrochloric Acid and 10% Formic Acid Methods from Cost Benefit Analysis

Benefit analysis, also known as cost benefit analysis, is a practical tool for estimating the profitability of a project by analyzing comprehensively, requiring an in-depth and thorough review.

Table 8. CBA estimation of 10% hydrochloric acid and 10% formic acid

Methods	Benefit Equivalent Annual	Annual Equivalent Cost	Ratio B/C
Acidizing Stimulation (10% Chloride)	2170591.816	1253433.996	1.731
Acidizing Stimulation (10% Formate)	1940631.429	1037913.564	1.869

- Annual Equivalent Benefit of Acidizing Stimulation (Chloride 10%) AEB = 2170591.816 US$ and Stimulation Acidizing (Formate 10%) AEB = 1940631.429 US$.

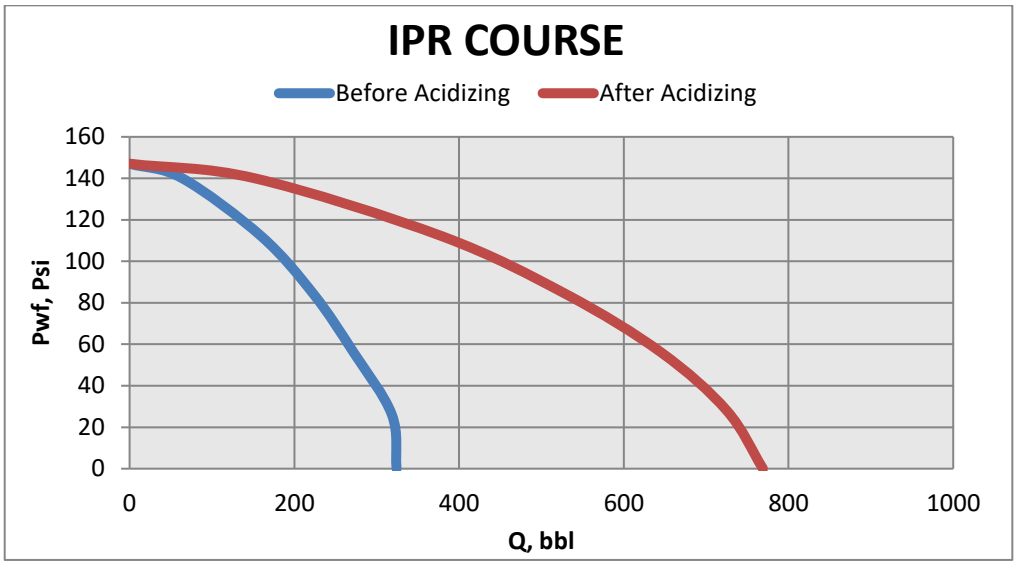

Figure 1. IPR Curves Before and After Acidizing Stimulation

- Annual Equivalent Cost of Acidizing Stimulation (10% Chloride) AEC 1253433.996 US$ and Stimulation Acidizing (Formate 10%) AEC =1037913.564 US$

Comparing the Acidizing Stimulation (Formate 10%) method with the 0 "Do Nothing" method. The increase in benefits from method 0 to the Stimulation Acidizing (Formate 10%) method is 1940631.429 US$ and the increase in costs is 1037913.564 US$. Thus the B/C ratio of the increase is

$$B/C_{B-0} = \frac{1940631.429}{1037913.564} = 1.9$$

$B/C_{B-0} > 1$, then the Acidizing Stimulation method (Formiat 10%) is selected, then the Acidizing Stimulation method (Formiat 10%) is compared with the Acidizing Stimulation method (Chloride 10%), so that the B/C ratio is increased as follows

$$B/C_{A-B} = \frac{\text{Benefit Equivalent A} - \text{Benefit Equivalent B}}{\text{Cost Equivalent A} - \text{Cost Equivalent B}}$$

$$= \frac{2170591.816 - 190631.429}{1253433.996 - 1037913.564} = 1.1$$

From this it can be concluded that the Acidizing Stimulation method (10% formate) is the best than the Acidizing Stimulation method (10% chloride), so Acidizing Stimulation (10% formate), which is chosen, in summary the selection of methods can be seen in **Table 9** below.

Table 9. Summary of Method Selection

Methods	Annual Benefits	Annual Cost	ΔA/ΔB ratio	Decision
B-0	1940631.429	1037913.564	1.9	Formate (10%)
A-B	229960.388	215520.432	1.1	Formate (10%)

IV. CONCLUSION

1. Well Z formed a $CaCO_3$ scale of 8.34 meq/lt and a $CaSO_4$ scale of 0.01 meq/lt which were analyzed based on physical data and chemical content of formation water obtained from the laboratory.
2. To overcome the scale problem, acidizing stimulation was carried out at a depth of 870 ft with 35 liters of mutual solvent, 101 liters of acid + chorotion inhobitor with injected acid volume of 60 bbl.
3. After acidizing stimulation, the average production of well Z has increased, based on the Productivity Index (PI) after acidizing stimulation has increased from 4.748 bbl/psi to 9.036 bbl/psi. The results of the Inflow Performance Relationship (IPR) curve reading, before acidizing the maximum flow rate (Q max) = 324,107 bpd, increased to Qmax = 769,021 bpd.

4. Based on the Cost Benefit Analysis (CBA), the Acidizing Stimulation method (10% formate) was chosen to overcome the scale problem because the B/C ratio >1 or 1.9 means that for every 1 US$ invested in the Acidizing Stimulation method (10% formate), a savings ratio o f 1.9 will be obtained. So it is very reasonable to decide that the Acidizing Stimulation method (10% formate), is feasible and more useful and efficient.

REFERENCES

Agusandi, D. P. (2017). Evaluation of Scale Problems of Wells SA-33, SA-101, SA-104 and SA-108 at PT Pertamina EP Asset 1 Field Ramba. Patra Akademika Engineering.

Anisa M., & Sudibjo, R. (2015). Analysis of Acidification Planning in JRR-2 and JRR-4 Wells in Field Y. National Seminar of Scholars.

Chen, L., (2018) Comparative Study Of Mechanical Removal Methods For Scale Deposites in Pipeline, Internasional Conference On Mechanical Engineering Proceedings.

Diky Pranondo, A. S. (2017). Evaluation of Sacle Problems of Well SA-33, SA-101. SA-104 and SA-108 at PT Pertamina EP Asset Fiels Ramba, Volume 08.

Henk Subekti, A. S. (2022). Evaluation of Scaling Potential on Production Pipe in Tapen Field PT Pertamina EP Asset 4 Field Cepu. SNTEM, Volume 2.

Kinasih, R. C. (2013). Analysis of Acidizing Treatment Results to Overcome Caco3 Scale in an Effort to Optimize the Production Capability of R-11 Wells PT. Pertamina EP asset 2 Limau Field. Mining Engineering.

Mety, Anisa and Rachat, S. (2015) Acidification Analysis of JRR-2 and JRR-4 Wells in Field Y. National Seminar of Scholars.

Muhammad, A. F. (2020). Analysis of the Success of Bullhead Method Acid Stimulation in the Heavy Oil Field of PT Chevron Pacific Indonesia.Petroleum Engineering Thesis, University of Riau.

Praditya, N., Leonardo, D. M., and Nur Wahyuni (2019). Case Study of Acidizing Matrix Design by Paying Attention to the Mechanism of Wormhole Formation in Carbonate Reservoirs. Journal of Mine Research. Volume 2.

Winsky. (2019). Cost/Benefit Analysis (CBA) Indonesia Risk Management Professional Association. https://cyberwhale.co.id/wpcontent/uploads/2019/11/ Cost-or-Benefit-Analysis.pdf

JOURNAL OF PETROLEUM AND GEOTHERMAL TECHNOLOGY
ISSN: 2723-0988, e-ISSN: 2723-1496
Vol. 5 No. 1 2024

Analysis of the Use of Sand Pump Control Pumps in Overcoming Sand Problem in Sucker Rod Pump (SRP) in Sp Wells In the Kawengan Field

Putri Sopacua [1*)]
2) Oil and Gas Production Engineering, Ambon State Polytechnic
* corresponding email: sopacuaputri06@gmail.com

ABSTRACT

The sand problem is a common challenge in the oil and gas industry. PT Pertamina EP Asset 4 Cepu Field in the Kawengan Field has rock which is a ngrayoung formation and the type of sandstone can cause sand to enter into the well bour when oil is produced for a long time. Therefore, we need the right tool to be able to overcome the problem of sandiness. In this case PT Pertamina EP Asset 4 Cepu Field in the Kawengan Field uses a sand control pump in an effort to overcome the sand problem. Thus, this research was conducted by analyzing the appropriate pump size from the sand rate calculation, fluid flow rate before and after using the sand control pump, as well as economic analysis. The results of the pump size analysis show that the right pump size to use is 2 joint mud anchors. The results of the subsequent analysis show an increase in the rate of fluid production after using a sand control pump. The results of the economic analysis show that the use of a sand control pump on a sucker rod pump (SRP) in the SP well is feasible because it has economic value with an oil price of 45 US$ / bbl, an NPV of 221,709 USD is obtained, and project success (IRR) reaches 106 %, as well as the value of pay out time for 1.83 years.
Keywords: Economy, Flow Rate, Sand Problem, Sand Control Pump, Sand Rate.

I. INTRODUCTION

The sand problem is one of the main challenges for the oil and gas industry, especially in the upstream sector (Roslan, et al., 2010). In the oil world, especially in wells using the sucker-rod pump lifting method in SP wells, various problems are often encountered which can disrupt the fluid production process from the well. These problems include sand which can arise due to the age of the well, the production process being carried out continuously over a long period of time causes the quality of the oil to decrease, the presence of frictional forces and collisions by the fluid flow causing the flow rate to exceed the maximum limit of the critical flow rate. These problems also cause the tubing to leak and become an obstacle to oil flow, blockage at the bottom of the well, and disrupt pump performance until the pump stops producing. PT Pertamina EP Asset 4 Cepu Field in the Kawengan field also has fluid / crude oil characteristics which are HPPO (High Pour Point Oil) which is paraffinic, meaning it contains wax, which has a low octane value and straight chain alkanes. Kawengan Field itself, the rock is the ngrayoung formation with a type of sandstone. Therefore, if an oil well is produced for a long period of time, it will cause the sand layer to fall on the oil layer so that sand can also enter the wellbore. If this sand is allowed to enter the pump, it will disrupt the performance of the pump itself and cause the pump to get stuck. Apart from that, the large amount of sand that is produced at various depths of certain wells in the Kawengan Field will cause a high frequency of well service. So to resolve sand in oil wells that contain a lot of sand and to increase the efficiency of the most effective pump, use low energy, and have low costs, a sand control pump can be used. Sand control pump is a process for removing sand contained in a well, in the form of a barrel and installed on tubing and then inserted into the well. This research was conducted to analyze the use of sand control pumps in overcoming sand problems in sucker rod pumps (SRP) in SP wells in the field Kawengan, by analyzing the right pump size from sand rate calculations, fluid flow rates before and after using the sand control pump, as well as economic analysis.

II. METHODS

The research method used was field research. The author collects the necessary data by requesting data or information from the petroleum engineer and discussing matters directly with the field supervisor regarding matters related to the research. The data required includes well profile data and sandrate data to explain the height of the sand falling on the liner. Well production data is needed to see usage before and after using sand pump control. Economic data is used to assess whether the investment made is feasible or not.

III. RESULTS AND DISCUSSION

Sand which is produced at the same time as oil is a problem that is often experienced in the world of oil. This can result in a decrease in the quality of production carried out. In addition, the production of sand can cause damage to well production equipment such as pumps. Therefore, choosing the right pump to use can minimize sand problems. In the process of selecting the right pump, it is necessary to analyze the right size to be used. Apart from that, it is also necessary to look at the comparison before and after using the pump, as well as the feasibility of using the pump from an economic perspective. PT Pertamina EP Asset 4 Cepu Field in Kawengan Field uses a sand control pump in an effort to overcome the sand problem.

Field Data Preparation

The data collection stage is a very vital activity to ensure the output that will be obtained as well. The most appropriate technique for obtaining results that are similar to actual field conditions. The data required includes well profile and sand rate data, well production data before and after using the sand control pump, as well as economic data by looking at NPV (Net Present Value), IRR (Internal Rate of Return), and POT (Pay out Time).

Sandrate Calculation Data

Produksi		Lama Produksi	Gross Total	Gross	Kedalaman	Kedalaman	Volume pasir pada	Debit pasir	Volume
Awal	Akhir	(t)	(TG)	(G)	Akhir PPS	Akhir PPS	liner 5,5"	(Qpasir)	pasir/m^3 fluida
		days	m^3	m^3/day	m		m^3	m^3/day	
06-Jan-19	15-Mar-19	69	1086	15,739	622	596	0,330774912	0,004793839	0,0003046
22-Mar-19	24-May-19	64	923,2	14,425	620	600	0,25444224	0,00397566	0,0002756
28-May-19	06-Aug-19	71	1093,4	15,400	608	603	0,06361056	0,000895923	0,0000582
11-Aug-19	27-Jan-20	170	2621,3	15,419	609,5	593,3	0,206098214	0,001212342	0,0000786
03-Feb-20	31-Mar-20	58	960,8	16,566	621	595	0,330774912	0,005703016	0,0003443
06-Apr-20	05-Jun-20	61	1225,9	20,097	620	600	0,25444224	0,004171184	0,0002076
11-Jun-20	11-Aug-20	62	1187,7	19,156	622	598,5	0,298969632	0,004822091	0,0002517
15-Aug-20	20-Oct-20	67	1320,9	19,715	622	595	0,343497024	0,005126821	0,0002600
26-Oct-20	07-Jan-21	74	1431,5	19,345	620	597	0,292608576	0,00395417	0,0002044
14-Jan-21	16-Mar-21	62	1102,5	17,782	622	604	0,228998016	0,003693516	0,0002077
18-Mar-21	19-Apr-21	33	562,4	17,042	616,5	596,5	0,25444224	0,007710371	0,0004524
23-Apr-21	09-May-21	17	326,9	19,229	609,5	591	0,235359072	0,013844651	0,0007200
13-May-21	05-Jul-21	54	900,9	16,683	622	598,5	0,298969632	0,005536475	0,0003319
12-Jul-21	08-Oct-21	89	1156,7	12,997	620	596	0,305330688	0,003430682	0,0002640
12-Oct-21	25-Nov-21	45	739	16,422	622	595,5	0,337135968	0,00749191	0,0004562
Total		996	16639,1	256,018			4,035453926	0,076362653	0,0044171
rata - rata				17,1				0,005090844	

Figure 1. Well Production Data (Before Using the Sand Control Pump

The sand height at the MA is assumed to be on January 11, 2022

- Volume of sand sucked in by the pump
  = Volume of sand/m^3 of fluid × TG until January 11th. 2022 × %puff……..……..(1)
  = 0.00024 x 790 x 55,88%
  = 0.10707 m^3

- Efficiency of pump filters

Because the Sand Control Pump has a filter in the intake channel, which functions to prevent the amount of sand being sucked in by the pump. So the filter efficiency is obtained at :

$L_{penampang} = \pi \times d_{in} \times filter\ length$……..…… …….(2)

$L_{hole} = \frac{\pi}{4} \times d_{mm} \times$ number of holes…… ……....……..……..…… (3)

Eff filter $= \frac{L_{penampang} - L_{hole}}{L_{penampang}} \times 100\%$……..……..……..……..……...(4)

Eff filter $= \frac{((\pi \times 4" \times 25{,}4 \times 260) - (\frac{\pi}{4} \times 5^2 \times 1026))}{\pi \times 4" \times 25{,}4 \times 260} \times 100\%$

Eff filter = 76%

- Volume of sand entering as of January 11th. 2022
  Vsand entering MA = Vsand sucked in by the pump x (1-Eff filter) ……..…… ……..(5)
  Vsand entering MA = 0,10707 x (1-76%)
  Vsand entering MA = 0,02599 m^3

- Sand height at MA as of January 11th. 2022

Sand height at MA $= \frac{V_{sand\ entering\ MA}}{L_{penampang\ MA}}$…… ……....……..……..……..…… (6)

Sand height at MA $= \frac{0{,}2599}{\frac{\pi}{4} \times d_{in}^2}$

Sand height at MA $= \frac{0{,}2599}{\frac{\pi}{4} \times (2{,}441 \times 0{,}0254)^2}$

Sand height at MA = 8,61 m

The height of sand that can enter the MA until January 11th. 2022 is 8,61 meters

Sand level on the liner as of January 11th. 2022

- Volume of filtered sand = Volume of sand sucked in by the pump x Eff filter…… ……..(7)
  Volume of filtered sand = 0,10707 m^3 x 76%
  Volume of filtered sand = 0,08108 m^3
- Vsand is not sucked in = Vsand / m^3 of fluid x TG until 11-01-22 x % not sucked in…… ……(8)
  Vsand is not sucked in = 0.00024 m^3 x790 x 44.12%
  Vsand is not sucked in = 0.08452 m^3
- Vsand falls to the bottom of the liner =Volume of filtered sand+Vsand is not sucked in…… ……..(9)
  Vsand falls to the bottom of the liner = 0,08108 m^3 + 0,08452 m^3
  Vsand falls to the bottom of the liner = 0,16561 m^3
- Sand level on the liner as of January 11 2022
  Height of sand on liner= $\frac{V_{\text{sand falls to the bottom of the liner}}}{L_{\text{penampang liner}}}$ ……..(10)
  Height of sand on liner = $\frac{0{,}16561 m^3}{\frac{\pi}{4}\times d_{in}^2}$
  Height of sand on liner = $\frac{0{,}16561 m^3}{\frac{\pi}{4}\times(5{,}012\times 0{,}0254)^2}$
  Height of sand on liner =13,02 m

The height of the sand falling to the bottom of the liner until January 11 2022 is 13.02 meters. Based on this data, we can further analyze the right pump size to use.

Sand forecast meets MA

- Volume MA 3 joint
  $V_{MA} = \frac{\pi}{4} d_{in}^2 \times h$ ……. (11)
  $V_{MA} = \frac{\pi}{4}(2{,}441 \times 0{,}0254)^2 \times 25{,}8$
  V_{MA} = 0,077856 m^3
- Sand forecast meets MA (tMA)
  $t_{MA} = \frac{V_{MA}}{Q_{sand}\times \%_{puff}\times(1-Eff\ filter)}$ ……..(12)
  $t_{MA} = \frac{0{,}077856}{0{,}00509084 \times 55{,}88\% \times (1-76\%)}$
  $t_{MA} = 112{,}7\ day$

The volume of sand sucked in by the pump is 0.077856 m3 and falls into the MA, which will fill the MA joint on the 113th day after the well is produced again. Namely on May 4, 2022, to be precise.

Estimate sand that fills the liner to the end of the concatenation

- Volume of liner to end of concatenation
  $V_{liner} = \frac{\pi}{4} d_{in}^2 \times h$ ……..(13)
  $V_{liner} = \frac{\pi}{4}(5{,}012 \times 0{,}0254)^2 \times (620 - 594{,}3)$
  $V_{liner} = 0{,}326958\ m^3$
- Estimated that the sand in the liner will be accommodated up to the end of the concatenation
  $t_{liner} = \frac{V_{liner}}{(Q_{sand}\times \%_{falling\ sand})+(Q_{sand}\times \%_{puff}\times Eff\ filter)}$ ……..(14)
  $t_{liner} = \frac{0{,}326958}{(0{,}00509084\times 44{,}12\%)+(0{,}00509084\times 55{,}88\%\times 76\%)}$
  $t_{liner} = 74{,}3\ days$

The volume of sand accommodated in the liner is 0.326958 m3 where the height can reach the end of the pump series on the 74th day after the well is produced. That is exactly March 26, 2022.

Sand forecast meet MA

- Volume MA 2 joint
  $V_{MA} = \frac{\pi}{4} d_{in}^2 \times h$
  $V_{MA} = \frac{\pi}{4}(2{,}441 \times 0{,}0254)^2 \times 17{,}2$
  V_{MA} = 0,051904 m^3

- Sand forecast meets MA (tMA)

$$t_{MA} = \frac{V_{MA}}{Q_{sand} \times \%_{puff} \times (1 - Eff\ filter)}$$

$$t_{MA} = \frac{0{,}051904}{0{,}00509084 \times 55{,}88\% \times (1 - 76\%)}$$

t_{MA} = 75,2 days

So the sand that is sucked in by the pump and falls into the MA will fill the MA joint on the 75th day after the well is produced again. Namely on March 27, 2022, to be precise.

Estimated sand filling the liner to the end of the concatenation

- Liner volume to the end of the concatenation

$$V_{liner} = \frac{\pi}{4} d_{in}^2 \times h$$

$$V_{liner} = \frac{\pi}{4} (5{,}012 \times 0{,}0254)^2 \times (620 - 585{,}7)$$

$$V_{liner} = 0{,}436368 m^3$$

- Estimated that the sand in the liner will be accommodated up to the end of the concatenation

$$t_{liner} = \frac{V_{liner}}{(Q_{sand} \times \%_{falling\ sand}) + (Q_{sand} \times \%_{puff} \times Eff\ filter)}$$

$$t_{liner} = \frac{0{,}436368}{(0{,}00509084 \times 44{,}12\%) + (0{,}00509084 \times 55{,}88\% \times 76\%)}$$

t_{liner} = 99,2 days

So the sand collected in the liner can reach the end of the pump circuit on the 99th day after the well is produced. That is, to be precise, April 20 2022.

Based on the calculation results above, it can be seen that the estimated height of sand falling to the bottom of the liner until January 11 2022 is 13,02 meters. With a pump size, 2 joint mud anchors fill the liner in around 99 days, while 3 joint mud anchors take around 74 days. Judging from the large volume accommodated, 3 joint mud anchors > 2 joint mud anchors, but this has big consequences, because the installation of mud anchors with up to 3 joints is not correct. Because by installing long mud-anchors, the pump circuit can quickly become pinched by sand deposits that cannot be sucked up by the pump. Even if the pump circuit is forced to be unplugged, the pump circuit can break due to excessive tensile stress so that the pump will be damaged. Therefore, it is better to install 2 joints mud anchor.

Well Production Data

Table 2. Well Production Data Before and After using sand control pump

Production		Production Tme (t)	Before		After	
Start	End		Gross (BFPD)	Gross Total (BFPD)	Gross (BFPD)	Gross Total (BFPD)
06-Jan-19	15-Mar-19	69	98,7	6809,2	99,0	6834,2
22-Mar-19	25-May-19	64	90,4	5788,5	90,8	5809,7
28-May-19	06-Aug-19	71	97,8	6855,6	96,9	6880,8
11-Aug-19	27-Jan-20	170	98,4	16435,6	97,0	16495,8
03-Feb-20	31-Mar-20	58	105,7	6024,2	106,1	6046,3
06-Apr-20	05-Jun-20	61	126,0	7686,4	126,5	7714,6
11-Jun-20	11-Aug-20	62	120,1	7446,9	120,6	7474,2
15-Aug-20	20-Oct-20	67	123,6	8282,0	124,1	8312,4
26-Oct-20	7-Jan-21	74	123,0	8975,5	121,7	9008,4
14-Jan-21	16-Mar-21	62	109,7	6912,7	110,1	6938,0
18-Mar-21	19-Apr-21	33	106,9	3526,2	107,2	3539,2
23-Apr-21	09-May-21	17	120,6	2049,7	121,0	2057,2
13-May-21	05-Jul-21	54	104,6	5648,6	105,0	5669,4
12-Jul-21	08-Oct-21	89	81,5	7252,5	81,8	7279,1
12-Oct-21	25-nov-21	45	103,0	4633,5	103	4650,5

Based on the data above, it is known that before using the sand control pump the fluid flow rate produced was small, namely 1000 – 2000 m3/day, because it had a high amount of sand so blockages occurred in the pump, if this is left

unchecked it will cause the production rate to decrease further and reduce quality. fluid. After the SP well uses a sand control pump, the fluid flow rate produced increases, namely 5000 - 16000 bfpd, so that production capacity increases because the amount of sand in the pump decreases and blockages do not occur. Reducing the amount of sand when production takes place can reduce the frequency of well service, while reducing the frequency of well service means that the lifetime of the well increases. Thus, the work of this well service activity can be said to be successful because there can be an increase in fluid.

Parameter		Unit	Total	Pre-2019	2019	2020	2021	2022
Sales Oil		BBL	41.557,85	-	13.714,84	13.714,84	13.714,84	413,32
Oil Price		US$/BBL	180,00	-	45,00	45,00	45,00	45,00
Expenditure	Sunk Cost	US$	-	-	-	-	-	-
	Capex	US$	110.500,00	110.500,00	-	-	-	-
	Tangibel	US$	-	-	-	-	-	-
	Intangibel	US$	110.500,00	110.500,00	-	-	-	-
	Opex	US$	492.044,99	-	162.383,74	162.383,74	162.383,74	4.893,76
	ASR	US$	400,00	-	100,00	100,00	100,00	100,00
Total Expenditure		US$	492.444,99	-	162.483,74	162.483,74	162.483,74	4.993,76
Depresiasi		US$	-	-	-	-	-	-
Gross Revenue		US$	1.870.103,42	-	617.167,95	617.167,95	617.167,95	18.599,58
FTP	0,2	US$	374.020,68	-	123.433,59	123.433,59	123.433,59	3.719,92
Gross after FTP		US$	1.496.082,74	-	493.734,36	493.734,36	493.734,36	14.879,67
Cost Recovery Calculation								
Depresiasi		US$	-	-	-	-	-	-
Capex Intangible		US$	110.500,00	110.500,00	-	-	-	-
Opex		US$	492.044,99	-	162.383,74	162.383,74	162.383,74	4.893,76
ASR		US$	400,00	-	100,00	100,00	100,00	100,00
Expense to be Recovered		US$	602.944,99	110.500,00	162.483,74	162.483,74	162.483,74	4.993,76
Prev year Unrec Cost		US$	-	-	-	-	-	-
total		US$	602.944,99	110.500,00	162.483,74	162.483,74	162.483,74	4.993,76
Available Fund for CR		US$	1.496.082,74	-	493.734,36	493.734,36	493.734,36	14.879,67
Total Cost Recovery (paid this year)			492.444,99	-	162.483,74	162.483,74	162.483,74	4.993,76
Equity to be split			1.003.637,75	-	331.250,61	331.250,61	331.250,61	9.885,91
Contraktor								
FTP		US$	-	-	-	-	-	-
Equity		US$	716.884,11	-	236.607,58	236.607,58	236.607,58	7.061,36
DMO Volume		US$	333.947,04	-	110.208,56	110.208,56	110.208,56	3.321,35
DMO Free		US$	333.947,04	-	110.208,56	110.208,56	110.208,56	3.321,35
DMO Loss		US$	-	-	-	-	-	-
Taxable Income		US$	716.884,11	-	236.607,58	236.607,58	236.607,58	7.061,36
Tax		US$	315.429,01	-	104.107,34	104.107,34	104.107,34	3.107,00
Income after Tax		US$	401.455,10	-	132.500,25	132.500,25	132.500,25	3.954,36
Contractor Cash Flow Calculation								
Cash In		US$	1.209.329,10	-	399.091,33	399.091,33	399.091,33	12.055,12
Cash out		US$	918.374,00	110.500,00	266.591,08	266.591,08	266.591,08	8.100,76
Contractor Net Cash Flow		US$	290.955,10	- 110.500,00	132.500,25	132.500,25	132.500,25	3.954,36
Discount Factor		10%		1,10	1,10	1,21	1,33	1,46
Discounted Net Cash Flow		US$	231.754,84	- 100.454,55	120.454,77	109.504,33	99.549,40	2.700,88
Government Entitlement								
FTP		US$	374.020,68	-	123.433,59	123.433,59	123.433,59	3.719,92
Equity		US$	286.753,64	-	94.643,03	94.643,03	94.643,03	2.824,55
Tax		US$	315.429,01	-	104.107,34	104.107,34	104.107,34	3.107,00
GOI Take		US$	976.203,33	-	322.183,96	322.183,96	322.183,96	9.651,40
GOI Take percentage,%			52%		52%	52%	52%	52%

Parameter Keekonomian		
NPV @10% Kontraktor	221.709	USD
IRR @10% Kontraktor	106,50 %	%
POT	1,83	Tahun
Contractor Take	290.955	USD
GOI Take	976.203	USD
GOI Take Percentage	52,13 %	%

Figure 2. Economic Parameter Data

Based on the table above, the discount rate used is 10%. This project is feasible. So the NPV is obtained at 221.709 USD. This value can be said to be feasible because the NPV value is greater than zero so that a project that will be carried out by the company is feasible to be implemented. With project success (IRR) reaching 106%, the IRR value is already greater than the discount factor of 10% so it is decided that the investment is worth implementing. The pay out time value or return on investment invested will return after 1,83 years, at the end of 2019.

IV. CONCLUSION

From the results of the research and discussion related to the title of the thesis, the author draws the following conclusions:

1. The sand rate that causes potential downhole problems in wells is around 13,02 meters. The size of the pump used is 2 joint mud anchors, so that the concatenation is not pinched by high sand deposits and does not damage the pump.
2. In the comparison table before and after using the sand control pump, it can be seen that there was an increase in production rate of 1 barrel after using the sand control pump. so that, well service activities are successful because fluid increases can occur.
3. Based on the results of economic indicators on the SP well with an oil price of 45 US$ / bbl, the NPV was obtained at 221.709 USD. With project success (IRR) reaching 106%. The payout time is 1,83 years. From the three economic indicators, it can be concluded that SP wells obtain positive NPV and high IRR from the discount rate. so that the use of a sand control pump on a sucker rod pump (SRP) in SP wells is feasible because it has economic value.

REFERENCES

Ahmed, T. (2006). reservoir engineering handbook third edition. Burlington: Elsevier

Bergkvam R (2015) parametric sensitivity studies of gravel packing. (Master's theses).

Doust, H., & Sumner, H. S. (2007). petroleum systems in rift basins - a collective approach in southeast asian basins. Petroleum Geoscience, 13(2), 127–44.

Herawati, I., Novrianti, & Suyandi, A. (2015). evaluasi peningkatan produksi pada formasi sandstone sumur #h dan #p dengan perencanaan stimulasi pengasaman matriks (studi kasus lapangan falih). JEEE, 1-15

Hisham, F. B. (2015). a critical review on root cause analysis on gravel packing design and installation issues. Bandar Seri Iskandar: Universiti Teknologi Petronas.

Ikporo, B., & Sylvester, O. (2015). effect of sand invasion on oil well production: a case study of garon field in the niger delta. The International Journal Of Engineering And Science (IJES), 64-72

Isehunwa, S., & Farotade, A. (2010). sand failure mechanism and sanding parameters in niger delta oil reservoirs. International Journal of Engineering Science and Technology, 777-82

Jamil, N. F. (2011). production enhancement from sand control management. Perak: Universiti Teknologi Petronas

Mayokun, A. O. (2011). practical approach to effective sand prediction, control and management. Abuja, Nigeria: African University of science and Technology

Moehadi, M., 2010, fundamental of petroleum geology and explorations, Indonesia University

Roslan, M. R., Deris , M. N., Hafiz, M., Saebi, S., Afendy, M. N., & Munoz, I. (2010). Rigless through-tubing gravel pack for sand control in malaysia. World Oil .

Satyana, A.H., 2008, petroleum geology of indonesia, IAGI Professional Courses, Bali.

Sinaga, S.B.R. 2020. Bahan Ajar :Keekonomian Migas Edisi I. Tapanuli Tengah : Petroleum Engineering

JOURNAL OF PETROLEUM AND GEOTHERMAL TECHNOLOGY
ISSN: 2723-0988, e-ISSN: 2723-1496
Vol. 5 No. 1 2024

Integration of 3G Data (Geomagnetic, Gravity and Geology) to Identify Geothermal System Controlled by Geological Structure of Telomoyo Plateau (Study Case Of Candi Umbul Area)

Boy Utama Bukit[1*)]
[2)] GeophysicalEngineering, Universitas Pembangunan Nasional Veteran Yogyakarta
*corresponding email: 115200022@student.upnyk.ac.id

ABSTRACT

As the technology development, there are more and more new innovations that utilize existing resources to support the energy needs and to fulfill the consumer needs. The energy source that is being discussed at this time is geothermal energy. Geothermal energy sources are considered effective because they are renewable and environmentally friendly when compared to other energies such as fossil energy. In Indonesia itself, geologically, it has a complex series of volcanoes that can be used as a heat source in this new energy innovation. One area that thought to have geothermal potential is the telomoyo mountain area, which is indicated by the manifestation of hot springs on the surface, precisely around Candi Umbul. However, it is necessary to conduct subsurface studies to identify the presence of subsurface structures such as faults or intrusions as heat sources, where this can be overcome using geophysical methods. This research was conducted using the integration of two geophysical methods, namely the geomagnetic method to determine the direction of the fault continuity and the gravity method to determine the regional heat source, and in the other side geological data as a reference for interpretation. From geomagnetic measurements, 163 rock magnetism data were obtained which indicated the existence of a fault continuity with northeast-southwest orientation in the direction of the river flow and cut the manifestation of hot springs. Meanwhile, from 176 gravity topex data, a high complete boguer anomaly value was obtained as an indication of an intrusion in the northeast that was cut by the fault recorded in the geomagnetic data. Based on geophysical data analysis and correlation with geological data from previous studies, it can be assumed that there is a geothermal system in the study area with andesitic intrusion as the heat source, fault structure with northeast-southwest orientation as a weak zone for meteoric water migration, andesite lava as caprock, unit tuff rock as a reservoir and the telomoyo plateau as a recharge area to supply meteoric water from the geothermal system.
Keywords: Geology, Geomagnetic, Geothermal, Gravity, Structure, Candi Umbul

I. INTRODUCTION

Along with the development of the times the need for energy is getting higher, while on the other hand the availability of main energy in the form of fossils is currently decreasing. Non-renewable fossil energy sources and complex prospecting areas encourage scientists to take advantage of existing technologies and resources.On the other hand, fossil-based energy is also not environmentally friendly because burning fossil fuels produces CO2 gas which can cause global warming (Jumina, & Wijaya, 2012). Responding to various problems in the energy industry, a new breakthrough is needed that can replace this energy and is environmentally friendly. Recently, a new and renewable energy source is known, namely geothermal energy. Geothermal energy is energy that utilizes geothermal heat to heat subsurface fluids and use it to drive turbines to generate electricity.

From a geological point of view, Indonesia is located at the confluence of three large plates (Eurasia, Indies-Australia and the Pacific) which causes Indonesia to have a complex tectonic setting. Subduction between continental and oceanic plates results in a magma smelting process in the form of partial melting. Mantle rock and magma undergo differentiation on their way to the surface. This process forms pockets of magma that play a role in the formation of volcanic pathways known as rings of fire. This has resulted in the emergence of a series of volcanoes in parts of Indonesia and their tectonic activities (Basid, A. 2014). This is certainly a very favorable condition for developing the geothermal energy industry as an environmentally friendly future energy source.

One of the areas in Indonesia that has geothermal energy potential is the Telomoyo area, Magelang, Central Java which is characterized by the manifestation of hot water on the surface. This is a topic that attracts geoscientists to conduct further research. One way that can be done in delineating the geothermal prospect zone is the geophysical method. The geophysical method itself has various methods that can identify the geological conditions of subsurface rocks, including the gravity method and the geomagnetic method. The gravity method utilizes variations in the density of subsurface rock and its distance to the surface which will affect instrument readings. The geomagnetic method is able to identify the distribution of the magnetic value of rocks which is influenced by various physical factors below the surface such as faults that cause the magnetism of subsurface rocks to decrease. Both of these methods can be integrated and linked with existing geological data so as to identify how the subsurface conditions are in analyzing geothermal systems such as heat sources and faults.

II. METHODS

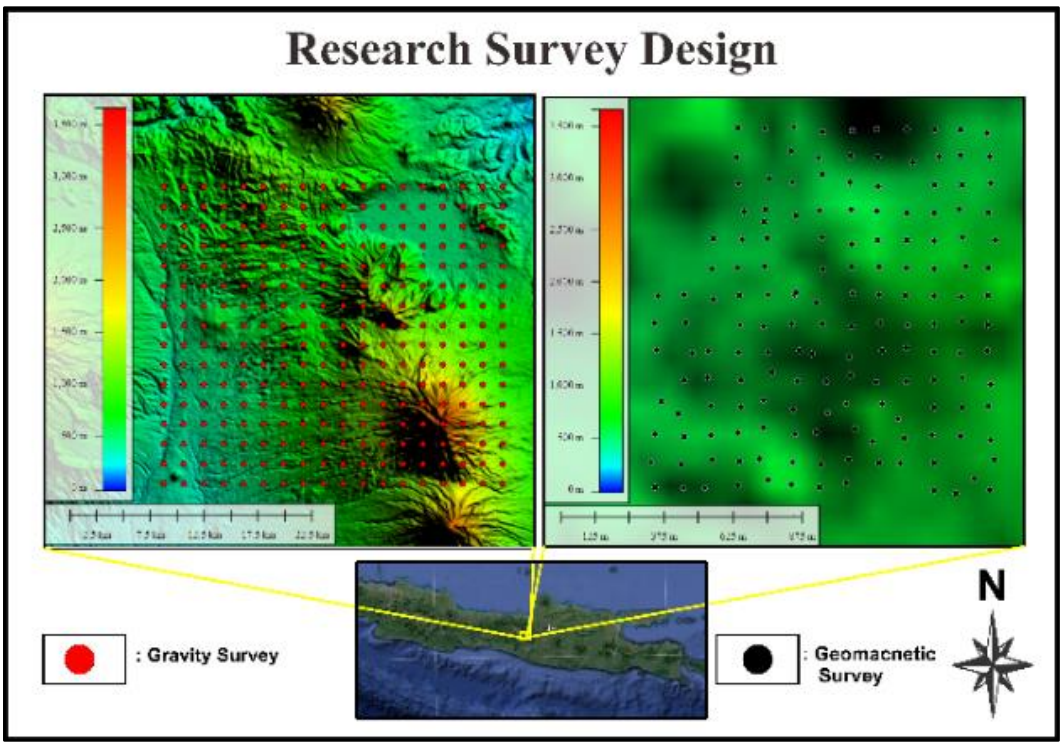

Figure 1. Reaserch survey design

The picture above is a geomagnetic survey design map using the gridding method which was carried out in the Candi Umbul Area, Grabag, Magelang, Central Java with a total of 164 measurement points. This research was conductedon the 12th and 13th of March 2022. The area of the research plot based on the survey design is 3.75 km2 with a length of 1.5 km and a width of 1.5 km. There are 14 measurement paths with a total of 14 acquisition points per trajectory. Measurement activities are carried out with the base rover concept using 3 PPM tools of the G-857 type where there is one tool that stays at a point (base) which is considered to have the least noise for correction of daily magnetic field variations later and one other tool moves according to the location of the measurement point.

In addition to the geomagnetic method, research is also carried out using the gravity method obtained from TOPEX satellite data. The TOPEX data obtained are in the form of elevation data and free air anomaly (FAA) values. TOPEX data acquisition reaches an area of 30 Km by 30 Km with the number of measurement points reaching 288 points with a space between points as far as 1800 meters. These two methods are then supported by geological data based on previous research.

Data processing from the two methods was carried out using Microsoft Excel and Oasis Montaj software. especially gravity data, processing is carried out through global mapper software to make field corrections after boguer corrections are carried out so that ABL values are obtained which can be further processed with Ipward, THD and TDR filters. Meanwhile, the obtained geomagnetic acquisition data is processed to obtain the value of Ha or the value of the magnetic intensity which is then performed with a Reduce to Pole (RTP) filter to obtain an RTP map that has been corrected for the influence of the main magnetic field from the earth which is dipole. RTP values that have been obtained can be further processed in the form of Lowpass, RTP and THD filters. Each value obtained from the gravity and geimagnetic methods is made into a map to facilitate the interpretation stage.

III. RESULTS AND DISCUSSION

3.1. Basic Theory Of Gravity

In 1687, Newton published Philosophiae Naturalis Principia Mathematica, which, among other things, stated Newton's law of gravitational attraction, where the magnitude of the gravitational force between two masses is proportional to each mass and inversely proportional to the square of their distance. In Cartesian coordinates, it can be displayed as shown below (Blakely et al, 1995).

JOURNAL OF PETROLEUM AND GEOTHERMAL TECHNOLOGY
ISSN: 2723-0988, e-ISSN: 2723-1496
Vol. 5 No. 1 2024

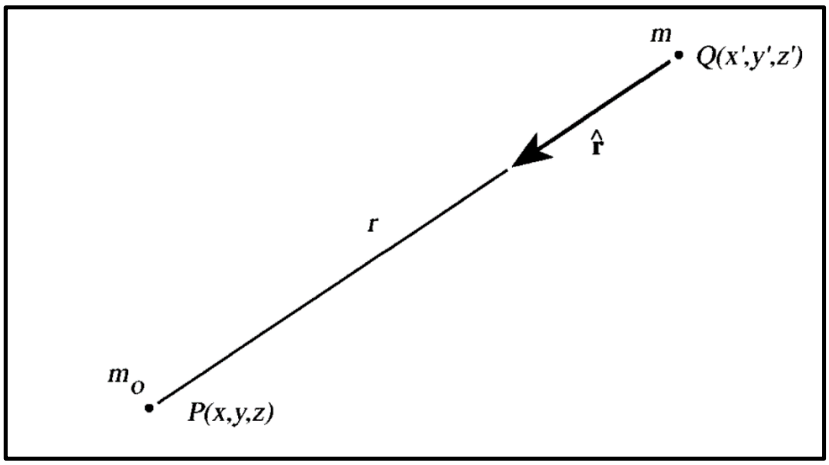

Figure 2. The masses m and mo experience a mutual gravitational force. By convention, the unit vector r is directed from the gravity source to the observation point, which in this case is located at the test mass m_0. (Blakely et al, 1995).

Theoretically, the magnitude of the force that works is formulated as follows;

$$\vec{F} = -G \frac{m_0 m}{r^2} \hat{r} \quad (1)$$

Where :
F ¯ = F between Object 1 and Object 2 (Newton)
m_0 = Mass of object 1
m_ = Massa of object 2
G = Gravitational Constant (6,672 x 10 -11 Nm / kg)
r = Distance between object 1 and object 2 (m)
rˆ = Unit vector from direction m to m0

3.2. Identification Of Fault Structures

One of the components in the geothermal system is a fault. Faults found below the surface, either normal faults or rising faults, can be a path for subsurface fluid migration from the surface to the heat source, or from the reservoir to the surface as a manifestation. Faults under the earth's surface are difficult to identify because not all of them are exposed on the surface. However, in this study, the presence of subsurface faults was identified using the geomagnetic method in the Candi Umbul area. Geomagnetic data survey was carried out in this area due to the presence of two manifestation points in the form of hot springs that were found and of course caused by the presence of a fault.

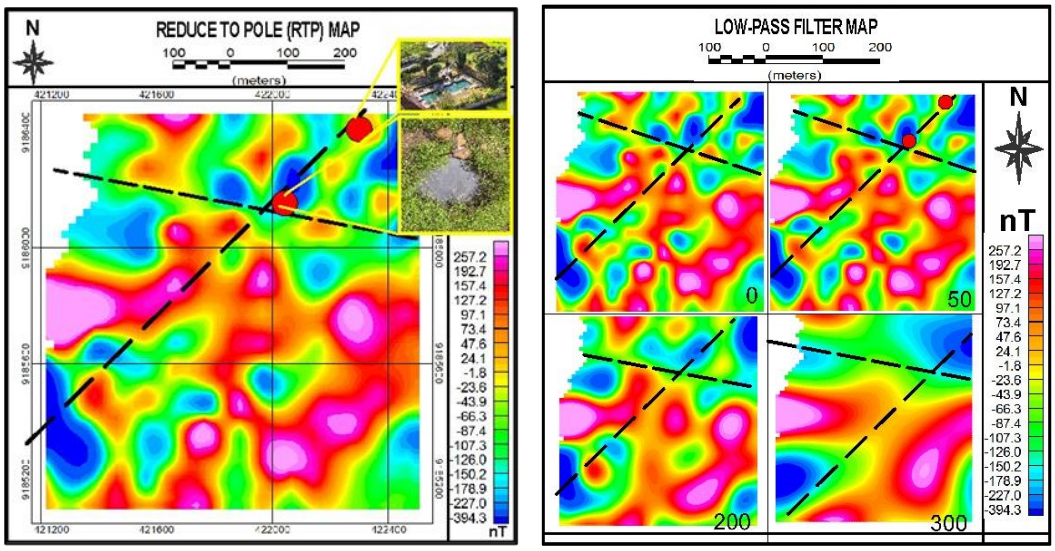

Figure 3. Reduce to pole map (top) and Low-pass filter map (buttom).

In the measurement of geomagnetic data in the field, the anomaly value obtained is the magnetic anomaly value in the research area. magnetic field (HA) which is then processed to produce a magnetic value that has been removed from the influence of the earth's dipole properties by using a reduce to pole filter. This filter causes the magnetic properties to become monopole so that the magnetic field displayed is the value of the magnetism that is right below it. On the RTP map, it can be seen that there are suspected faults with NE-SW and EW directions which are characterized by low and continuous anomalies. In addition to separating local and regional anomalies from the obtained magnetic values, use a low pass filter. This filter only captures low-frequency values so that it gives the results of the response of rocks that are far from the surface. The lowpass filter map also shows the alleged presence of a fault with the same direction as the previous assumption. This shows that the fault structure in the study area is a regional fault as well.

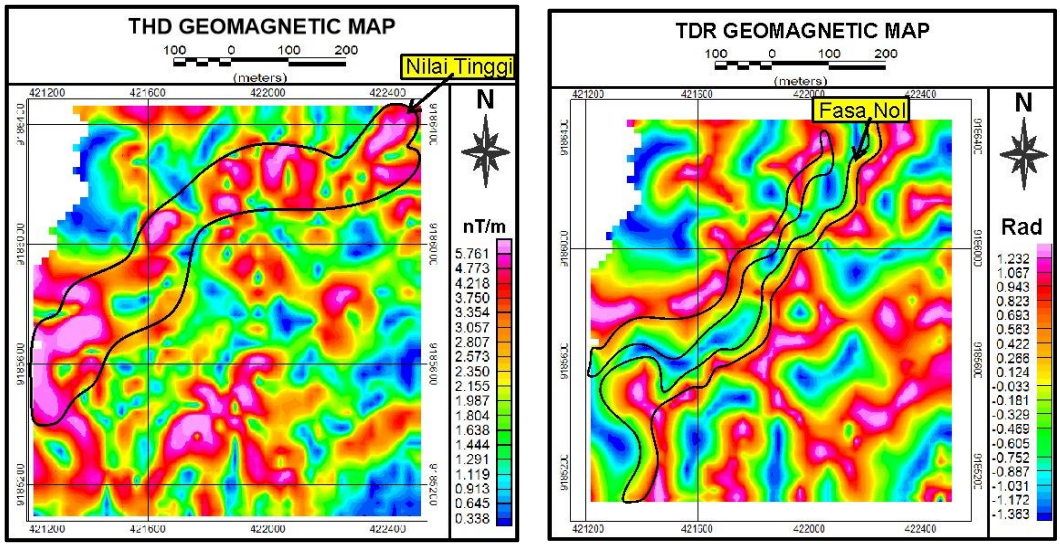

Figure 4. THD geomacnetic map (top) and TDR geomacnetic map (bottom).

The assumption of the existence of this fault is reinforced by data from the THD and TDR filters which can be seen on the THD and TDR maps. The THD value is obtained from the derivation of the RTP value. in principle, the THD value will be high at the boundaries of the anomaly, so this filter can be applied to the determination of fault boundaries in the study area. On the THD map it can be seen that the previously predicted fault position has a high value along its side. On the map obtained, it can be seen that the fault structure with a NE-SW direction shows high values as indicated by the white line. Meanwhile, a high THD value is also shown in the fault in the EW direction. Unlike the THD filter, the TDR filter has the principle that the anomaly value will be zero when it is at the anomaly boundary. on the map it can be seen that the position of the alleged fault gives an anomalous response with a value of zero which is continuous along the side of the fault. this indicates that the zero anomaly value indicated by the white line in the figure is the boundary of the fault. The sharpening of this anomaly strengthens the assumption that the fault has a NE-SW direction and a NW direction.

The identification of the next fault structure can be seen from the boundary of the anomaly and the body of the fault. Where to see the section, the Total Horizontal Derrivative (THD) and Tilt Derrivative (TDR) filters are used to identify the presence of the structure by looking at the boundaries and body of the fault. In the **Figure 3.** the map on the top is the result of the Total Horizontal Derrivative (THD) filter and the Tilt Derrivative (TDR) filter on the buttom. Conceptually, the THD filter is a combination of the X and Y orientation First Horizontal Derivative analysis, where this filter raises the value at the anomaly boundary. While the TDR filter is a filter that is used to see the anomalous boundaries along with their geometric shapes and directions. If seen on the THD map, the boundaries of the anomalies indicated as structures in the form of northeast-southwest trending faults, the majority show high values along their continuity. Likewise with several minor faults that appear in a northwest-southeast direction, the boundaries of each fault line can be seen.

To see another form of the fault, it can be seen on the TDR map where the TDR map clarifies the boundary of the anomaly by looking at phase 0 on the entire map. Phase 0 here is shown in the yellow shutter where the orientation direction and geometric shape of the fault can be determined with this TDR map. It can be seen that the majority of phase 0 directions are in the northeast – southwest which describes the orientation direction of the northeast – southwest major fault. While a small part of phase 0 with a northwest-southeast orientation describes a minor fault formed in the study area.

With the support of the control structure in the form of a fault that appears on the RTP map and all of its filters (Lowpass, TDR, and THD) and based on the geological map data of the telomoyo area which shows the direction of the slump of the fault zones that cause geothermal manifestations, the structural aspect Geothermal control in the Telomoyo area is considered a prospect and is one aspect of the geothermal system that has been fulfilled.

Based on the geological data that has been obtained, the main lineage in the study area has an east-west orientation. This lineament is a characteristic of the Java structure that occurs due to the subduction of the Indo-Australian plate which moves towards the Eurasian plate to the north. On the other hand, there is also a fault structure that dominates the study area which is continuous in the NE-SW direction. This northeast-southwest pattern is indicated as a result of the formation of the Soropati mountain caldera. The direction of the continuity of the structure obtained can also be observed in the DEM data and the pattern of river water continuity on the surface. In addition, two points of manifestation in the form of hot springs that are connected also form a NE-SW orientation. this shows similar results to the obtained geomagnetic data. On the map, it can be seen that the east-west orientation lineage pattern in the north and the NE-SW pattern are shown by low anomalies. The type of fault that developed in the study area is a normal fault. This fault cuts the subsurface rock that acts as a reservoir and caprock so that the fluid comes to the surface as a manifestation in the form of hot springs as an outflow zone.

3.3. Heat Source Analysis

Apart from the manifestation of hot water and existing structures, other components in the geothermal system are heat sources or heat sources. The heat source of a hydrothermal system is generally in the form of an intrusion body or magma from volcanic activity. However, there are also sources of hydrothermal heat that are not derived from igneous rock but are generated from the uplift basement rock which is still hot or it can also come from tectonic activity in the form of faults and folds so that the rock circulation warms up. This difference in heat sources will have implications for differences in geothermal reservoir temperatures in general, will also have implications for differences in geothermal systems (Goff & Janik 2000). Apart from that, in general, the heat source must have a high density so that it gives a high gravity anomaly value as well.

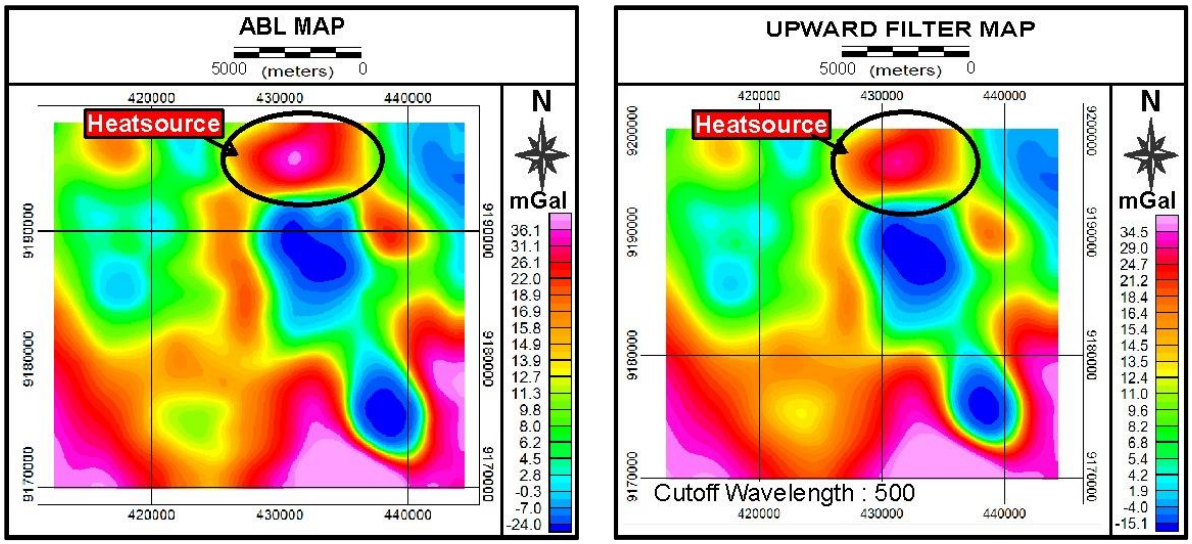

Figure 5. ABL map (top) and Upward filter map (buttom).

Based on the gravity data obtained, the distribution of the value of the gravity anomaly is influenced by the density factor and the distance between the subsurface formation and the surface. The picture above is a complete Boguer Anomaly (ABL) map (left) and an upward continuation filter map with a cut of wavelength value of 500. The ABL map can obtain information in the form of the distribution of subsurface gravity anomaly values at a point that has been corrected for factors affecting acceleration. gravity such as elevation, average density, latitude position, tides, high gravity anomaly value of the study area is in the southern part of the study which is indicated by red to ung with values of 10 mGal to 30 mGal which can be seen on the scale bar. However, there is also a high anomaly value in the northern part which forms a circular closure which is suspected as a heat source in the study area. the location of this intrusion is in the northern part of the caldera of Mount Soropati.

JOURNAL OF PETROLEUM AND GEOTHERMAL TECHNOLOGY
ISSN: 2723-0988, e-ISSN: 2723-1496
Vol. 5 No. 1 2024

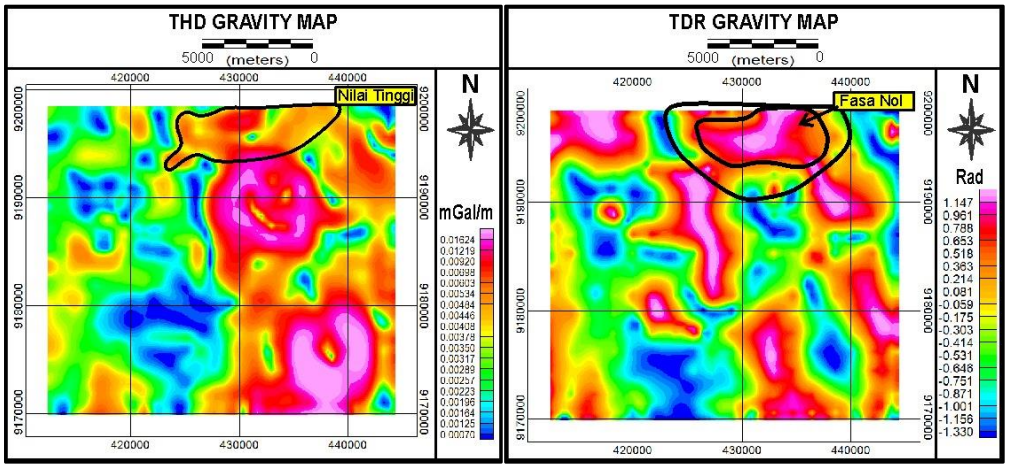

Figure 6. THD gravity map (top) and TDR gravity map (buttom).

The ABL value that has been obtained is then amplified by amplifying the signal through the Total Horizontal Derivative (THD) and Tilt Derrivative (TDR) filters. The THD map will elevate the boundaries of the anomaly. On the map we can see that the low and high anomaly boundaries that we have obtained previously produce high values on this THD map. The position of the previously suspected heatsource is further strengthened by the limits that can be seen with the THD value reaching 0.0164 mGal/m. however, the map tends to strengthen the low anomaly which is suspected to be the reservoir of the geothermal system. Unlike the TDR map, the boundaries of the anomaly will be shown with a value of zero. the anomalous boundaries on this map appear to be rounded and surround the predicted intrusion and reservoir locations.

From the geological data obtained, the rocks that make up the study area are dominated by volcanic rocks with heat source sourced from andesite-basaltic magma under the surface resulting from the vulcanization process of the Telomoyo volcano. This intrusion provides heat to the subsurface rock which is then in contact with the fluid in the reservoir so as to produce a fluid that has heat which then exits to the surface through a weak zone in the form of a normal fault that has been previously delineated.

3.4. Geothermal System Analysis

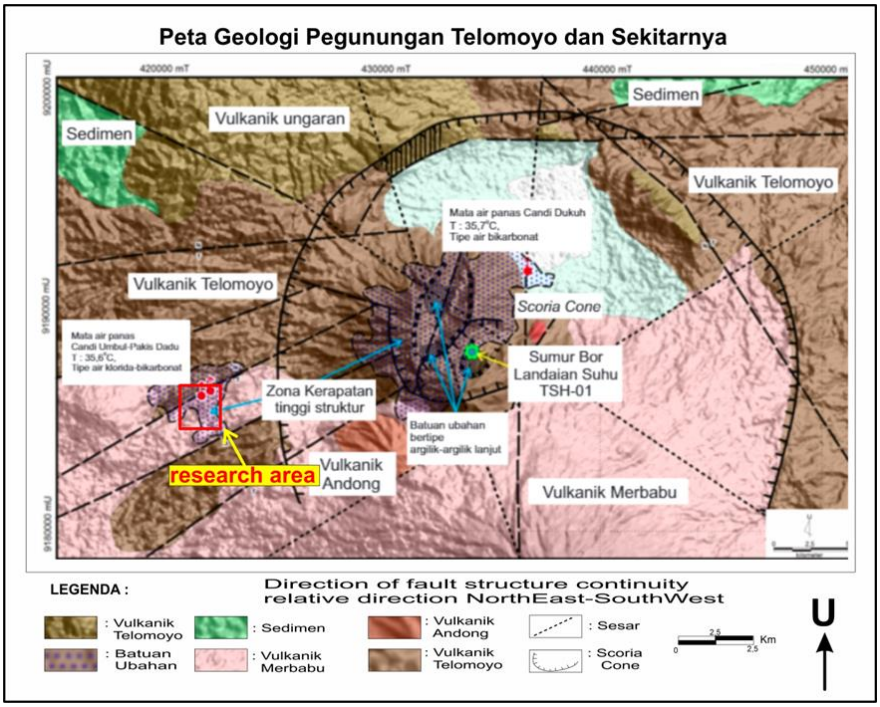

Figure 7. THD gravity map (top) and TDR gravity map (buttom).

Based on the analysis of research data that has been carried out and correlated with geological data from previous studies, information on geothermal systems is obtained which includes heat sources, reservoirs, overburden, faults and recharge areas. A geothermal field will not be able to stand if one of these components is not met. The components of the geothermal system that are the focus of this research are the presence of heat sources and fault structures as fluid migration paths in the Candi Umbul geothermal system.

From the data that obtained, the geothermal system in the area of Candi Umbul is a volcanic geothermal system consisting of a heat source component in the form of andesite magma intrusion, tuff as a reservoir, massive andesite lava as cap rock and the telomoyo mountains as a recharge area. Meteoric water enters the subsurface in the caldera of Mount Seropati through existing fractures to the reservoir in the form of tuff rock with good porosity and permeability values. The fluid is then heated by the andesite intrusion by conduction through the heated subsurface rock. Fluids that have experienced an increase in temperature are transported back to the surface through weak zones such as fractures and faults. In this condition, Fluid transport takes place through the Java fault with an east-west orientation and a normal fault caused by the Telomoyo volcanic activity in a NE-SW direction. The temperature and pressure in the reservoir are maintained due to the presence of overburden or clay cap in the form of andesite lava rock near the surface. In some locations, the fault cuts the claycap so that manifestations arise in the form of hot springs, and one of them is in the area of the Candi Umbul. From the various components that interact with each other in the research area, it is suspected that the Candi Umbul area has geothermal potential which can be developed into a source of electricity generation as an environmentally friendly and sustainable future energy defense effort. The temperature and pressure in the reservoir are maintained due to the presence of overburden or clay cap in the form of andesite lava rock near the surface. In some locations, the fault cuts the claycap so that manifestations arise in the form of hot springs, and one of them is in the area of the Candi Umbul. From the various components that interact with each other in the research area, it is suspected that the Candi Umbul area has geothermal potential which can be developed into a source of electricity generation as an environmentally friendly and sustainable future energy defense effort. The temperature and pressure in the reservoir are maintained due to the presence of overburden or clay cap in the form of andesite lava rock near the surface. In some locations, the fault cuts the claycap so that manifestations arise in the form of hot springs, and one of them is in the area of the Candi Umbul. From the various components that interact with each other in the research area, it is suspected that the Candi Umbul area has geothermal potential which can be developed into a source of electricity generation as an environmentally friendly and sustainable future energy defense effort.

IV. CONCLUSION

Based on the research that has been done, several conclusions were obtained as follows;

1. Variations in susceptibility values from the obtained geomagnetic data indicate a low and continuous magnetic field anomaly which indicates a structure in the form of a fault reinforced by a high value THD value and a zero phase TDR value with a NE-SW direction and an EW direction.
2. Complete Boguer Anomaly (ABL) data shows a suspected heat source in the Northeast of the study area which is indicated by high anomaly values and reinforced by THD maps with high values and TDR with zero phase values.
3. Geological data on the surface is in line with subsurface data in identifying components of the geothermal system which includes the heatsource in the northeast which is cut by a fault in the NE-SW direction which intersects two manifestations of hot water and is in the direction of river water flow. Other components of the geothermal system consist of andesite lava as caprock, andesite intrusion as heat source, tuff rock unit as reservoir and there is a normal fault structure as a weak zone for fluid migration as well as a recharge area zone from the telomoyo mountains.

ACKNOWLEDGEMENTS

We especially thank God The Almighty who has bestowed His grace and gifts so that researchers can complete a scientific work entitled " Integration of 3D Data (Geomagnetic, Gravity and Geology) to Identify Geothermal System Controlled by Geological Structure of Telomoyo Plateau (Study Case of Candi Umbul)". We also thank our beloved family, as well as the CONTINENTAL family of Geophysical Engineering UPN Veteran Yogyakarta batch 2020 that helped in obtaining field data as the basis for compiling this scientific paper, lastly we thank all parties who we cannot mention one by one in their efforts to help preparation of this scientific work.

REFERENCES

Agista, Zendi, et.al. 2014. *Analisis Litologi dan Struktur Geologi berdasarkan Citra Landsat pada Area Prospek Panasbumi Gunung Telomoyo dan Sekitarnya, Kabupaten Magelang, Provinsi Jawa Tengah.* Geological Engineering E-Journal, 6 (1): 278 – 293.

Basid, Abdul, Nita Andrini, & Sofi Arfiyaningsih. 2014. *ESTIMATION OF GEOTHERMAL SYSTEM RESERVOIR USING GEOELECTRICAL SURVEY, RESISTIVITY AND POTENTIAL SELF*. Neutrino Journal, 7(1), 57-70

Hermawan, Eddy. 2012. *Sistem Panas Bumi Daerah Candi Umbul, Telomoyo berdasarkan Kajian Geologi dan Geokimia.* Geological Resources Bulletin, Bandung: Geological Resource Center.

Hermawan, D dan Y. Rezky. 2011. *Delineasi Daerah Prospek Panas Bumi berdasarkan Analisis Kelurusan Citra Landsat di Candi Umbul – Telomoyo, Provinsi Jawa Tengah.* Geological Resources Bulletin, Bandung: Geological Resource Center.

Jumina & Wijaya, Karna. 2012. *PROSPECTS AND POTENTIAL RENEWABLE ENERGY RESOURCES (RES) IN INDONESIA.* UGM Center for Energy Studies : Yogyakarta.

Ramadhan, N., et.al. 2014. *Evaluasi Kondisi Geologi dan Geokimia Potensi Panas Bumi Gunungapi Telomoyo*. *Proceedings of the 7th National Earth Seminar*. Geological Engineering Department, Faculty of Engineering, Gadjah Mada University, October 30th – 31st 2014.

Reynolds, John M. 2011. *An Introduction to Applied and Environmental Geophysics Second Edition*. United Kingdom: John Wiley and Sons.

Telford, W. M., et.al. 1990. *Applied Geophysics Second Edition.* New York: Cambridge University.